Eur. Phys. J. C (2026) 86:235
https://doi.org/10.1140/epjc/s10052-026-15409-5

THE EUROPEAN PHYSICAL JOURNAL C

Regular Article - Theoretical Physics

Non-holomorphic contributions in GMSB with adjoint messengers

Büşra Niş[a], **Cem Salih Ün**[b]

Department of Physics, Bursa Uludağ University, 16059 Bursa, Turkey

Received: 22 August 2025 / Accepted: 7 February 2026
© The Author(s) 2026

Abstract We consider models of gauge mediated supersymmetry breaking involving the messenger fields from the adjoint representation of MSSM's gauge group. In addition, we include the non-holomorphic (NH) terms induced by the supersymmetry breaking and involve them in the renormalization group evolution in calculating the low scale implications. With the NH contributions, the stau mass-square can be driven to the positive values in the renormalization group evolution, even if the hypercharge interactions are small. We realize that the NH contributions can be as high as about 25 TeV in the right-handed stau mass. Despite such large contributions, the effects from the NH terms in sparticle mixing can lower the overall NH contributions in the mass eigenstates by about 5 TeV. Similarly, the sbottom mass can differ by about 6–7 TeV, and the stop mass by about 15 TeV, when the NH terms are largely induced. Their contributions in the sparticle masses lead to significant impacts in the SM-like Higgs boson as well. The NH contributions can yield 80 GeV heavier SM-like Higgs boson. In a small region of the parameter space, we also observe negative NH contributions in the masses such that the sparticles can be lighter about 1 TeV while the Higgs boson mass can be lowered by about 20 GeV in this region. The NH contributions can have interesting consequences in the muon anomalous magnetic moment (muon $g-2$). The NH terms reduce the supersymmetric contributions to muon $g-2$ by leading to heavier mass spectrum. In addition, the NH mixing term in smuons lowers further such that the light sleptons, neutralinos and charginos can still be consistent with the latest updates in muon $g-2$ measurements.

1 Introduction

In addition to completing the Standard Model (SM), the breakthrough discovery of the Higgs boson [1–3] is not only an observation of new particle, but it also defines and shape the path through the models beyond the SM (BSM). While the long standing problems of SM such as the gauge hierarchy problem, absence of dark matter (DM) have already led to the need for BSM, the detailed analyses on the Higgs boson have pointed out also new problems as the stability of the Higgs potential within SM [4–6]. Even the minimal supersymmetric extension of SM (MSSM), as being one of the appealing candidates for BSM by proposing a solution to the hierarchy problem, needs to heavy supersymmetric particles to accommodate a consistent Higgs boson in the mass spectrum [7,8] in the models based on the gravity mediated SUSY breaking or gauge mediated SUSY breaking (GMSB) scenarios. The impact from the 125 GeV Higgs boson mass becomes even severer in GMSB scenarios, since the mixing in the supersymmetric scalars is negligible. In this case, the SUSY spectrum needs to involve heavy sparticles ($\mathcal{O}(10)$ (TeV)) to accommodate the SM-like Higgs boson with a consistent mass [9,10].

The level of the sensitivity in the current experimental analyses in the Higgs boson mass ($\Delta m_h = \mathcal{O}(100)$ MeV) [11] requires also more sensitive calculations, which might be accomplished by matching conditions at different energy scales, fixed-point calculations [12] and/or considering radiative corrections from the higher order renormalization group equations (RGEs) [13,14]. Such improvements can shift the theoretical results of the Higgs boson mass up to about 3 GeV when the mixing among the stops is large [15]. On the other hand, in the models such as those in GMSB class, this shift cannot exceed about 0.5 GeV [16], since the mixing in stops is negligible in this class. In this context, despite being necessary, such contributions are not large enough to ameliorate

[a] e-mail: 501507008@ogr.uludag.edu.tr
[b] e-mail: cemsalihun@uludag.edu.tr (corresponding author)

Published online: 07 March 2026

the impact from the Higgs boson mass on the mass spectrum. Thus, one can also consider to extend the symmetry [17] and/or several messengers which carry SUSY breaking to the visible sector.

In our work, we consider a class of GMSB models which propose several messenger fields transmitting the SUSY breaking to the visible sector through the gauge interactions. One can construct such models with the messengers from the adjoint representation of the MSSM gauge group [18,19]. An incomplete version of these models allows to accommodate relatively light weakly interacting SUSY particles in the spectra, by splitting the sleptons from squarks, and it can lead to interesting implications which can be tested experimentally [20–22]. However, this version suffers from inconsistently light sleptons and needs to be extended to fit consistent masses for the charged sleptons [21,22].

In addition to consider the full representation for the messenger fields, we also invoke the contributions from some non-holomorphic (NH) terms in our analyses. Such terms are strictly forbidden by the holomorphy condition; however, they can be induced during the SUSY breaking [23–30]. The emergence of such terms might be a sign of hard SUSY breaking, and they can lead to the hierarchy problem if SUSY is broken through a VEV of a field which is singlet under MSSM gauge group. However, they can be listed as the soft supersymmetry breaking (SSB) terms in the absence of a MSSM singlet field [23,27–29]. Due to the holomorphy condition before the SUSY breaking, one needs to consider one loop further in the perturbation theory [30], and the dimensionality indicates a further suppression by $1/M$ in NH terms compared to the usual holomorphic SSB terms [25,27]. This suppression might be considered as to be the reason that these terms have been neglected mostly, but some recent studies have shown that the impact from these parameters can be considerable even when they are small at the SUSY breaking scale [31–40].

On the other hand, previous studies mostly consider the NH terms effectively by including them at the decoupling scale ($M_{\rm SUSY} \equiv \sqrt{m_{\tilde{t}_L} m_{\tilde{t}_R}}$, where $m_{\tilde{t}_L}$ and $m_{\tilde{t}_R}$ are the SSB masses of the left and right-handed stops, respectively). In these cases, the SSB terms evolve from a high scale to the electroweak scale without NH terms, and the NH effects rather emerge from the mixing of the sfermions and their couplings to the "wrong" Higgs field [30]. However, these contributions might be cancelled out if the SSB parameters and couplings evolve from a high scale together with the NH terms by the renormalization group equations (RGEs). In this way, one can also link the presence of NH terms to the SUSY breaking, as we follow in our analyses. The rest of the paper is organized as follows: We describe the models with the adjoint messengers in GMSB models (hereafter, GMSB-ADJ) by considering the induced SSB terms in Sect. 2. We also introduce the NH terms and their contributions to the observables in this section. Section 3 briefly summarize the data generation and experimental constraints employed in our analyses. We discuss our results for the fundamental parameter space of the models, the NH contributions to the mass spectra including the Higgs boson in Sect. 4. After the latest release about the experimental and theoretical results of muon anomalous magnetic moment (muon $g-2$), we also add a note about the NH impact on muon $g-2$ in Sect. 5. Finally we summarize and conclude our results in Sect. 6.

2 SSB with the adjoint messengers

In the GMSB models, the SUSY breaking is induced in the visible sector through the gauge interactions. The minimal models of this class usually consider the messengers resided in $\mathbf{5}+\bar{\mathbf{5}}$ representations of $SU(5)$ and/or $\mathbf{10}+\bar{\mathbf{10}}$ of $SO(10)$. Despite their nice flavour blind structures, these minimal models receive strong negative impact from the Higgs boson discovery [9,10,17,41–44]. Even though it is slightly away from the minimality, one can also consider several messengers resided in the adjoint representation of the MSSM gauge group. In these models of the GMSB-ADJ class, the messengers interact with a gauge singlet field $\hat{S} = S + \theta^\alpha \psi_\alpha + \theta^2 F$ in the hidden sector through the following superpotential:

$$W_{\rm ADJ} = (\mathcal{M}_5 + \lambda_5 \hat{S})\Sigma_5\Sigma_5 + (\mathcal{M}_3 + \lambda_3 \hat{S})\mathrm{TR}(\Sigma_3\Sigma_3) + (\mathcal{M}_8 + \lambda_8 \hat{S})\mathrm{TR}(\Sigma_8\Sigma_8), \quad (2.1)$$

where Σ_5, Σ_3 and Σ_8 represent the messenger fields which interact with the MSSM fields through $U(1)_Y$, $SU(2)_L$ and $SU(3)_C$, respectively. Note that Σ_5 in our notation corresponds to the fields in $\mathbf{5}+\bar{\mathbf{5}}$. Note that, the gauge singlet field $\hat{S}$ in this superpotential is not one of those taking part in hard breaking of SUSY, since it does not interact with the MSSM fields directly. The terms $\mathcal{M}_5$, $\mathcal{M}_3$ and $\mathcal{M}_8$ stand for masses of the messenger fields, and, for simplicity, they are set to be equal in our analyses as $\mathcal{M}_5 = \mathcal{M}_3 = \mathcal{M}_8 \equiv M_{\rm Mess}$, which is expected to be at the order of $\langle S \rangle$. SUSY breaking VEV of $\hat{S}$ can be expressed in terms of its scalar components as $\langle \hat{S} \rangle = \langle S \rangle + \theta^2 \langle F \rangle$, which induces different masses for the bosonic and fermionic components of the messenger fields as

$$m_{b_i} = M_{\rm Mess}\sqrt{1 \pm \frac{\Lambda_i}{M_{\rm Mess}}}, \quad m_{f_i} = M_{\rm Mess}, \quad i = 5, 3, 8; \quad (2.2)$$

where $\Lambda \equiv \lambda_i \langle F \rangle / M_{\rm Mess}$. As seen from the mass expression of the bosonic component, the condition $\Lambda_i < M_{\rm Mess}$ should hold to avoid tachyonic states ($m^2_{b_i} < 0$). The SSB masses for the gauginos and the matter fields emerge in the same way as described for the minimal GMSB models: i.e. the SSB gaugino masses at one-loop and the scalar masses at two-loop [45]. In the case of the adjoint messengers, the SSB

masses can be derived [19] for the gauginos as

$$M_1 \simeq \frac{g_1^2}{16\pi^2}(5\Lambda_5), \qquad M_2 \simeq \frac{g_2^2}{16\pi^2}(2\Lambda_3+3\Lambda_5), \quad \text{(2.3-a)}$$
$$M_3 \simeq \frac{g_3^2}{16\pi^2}(3\Lambda_8+2\Lambda_5),$$

and for the sfermions

$$\begin{aligned}
m_Q^2 &\simeq \frac{2}{(16\pi^2)^2}\left[\frac{4}{3}g_3^4(3\Lambda_8^2+2\Lambda_5^2)+\frac{3}{4}g_2^4(2\Lambda_3^2+3\Lambda_5^2)\right.\\
&\quad \left.+\frac{3}{5}g_1^4(5\Lambda_5^2)\frac{1}{6^2}\right]\\
m_U^2 &\simeq \frac{2}{(16\pi^2)^2}\left[\frac{4}{3}g_3^4(3\Lambda_8^2+2\Lambda_5^2)+\frac{3}{5}g_1^4(5\Lambda_5^2)\left(\frac{2}{3}\right)^2\right]\\
m_D^2 &\simeq \frac{2}{(16\pi^2)^2}\left[\frac{4}{3}g_3^4(3\Lambda_8^2+2\Lambda_5^2)+\frac{3}{5}g_1^4(5\Lambda_5^2)\frac{2}{3^2}\right]\\
m_L^2 &\simeq \frac{2}{(16\pi^2)^2}\left[\frac{3}{4}g_2^4(2\Lambda_3^2+3\Lambda_5^2)+\frac{3}{5}g_1^4(5\Lambda_5^2)\frac{1}{2^2}\right];\\
m_{H_u}^2 &= m_{H_d}^2 = m_L^2\\
m_E^2 &\simeq \frac{2}{(16\pi^2)^2}\left[\frac{3}{5}g_1^4(5\Lambda_5^2)\right].
\end{aligned} \quad \text{(2.3-b)}$$

As happens in the GMSB models, the trilinear SSB couplings can be induced at the third-loop and so they are suppressed by an extra $M_{\rm Mess}$ factor. Thus they can be set to zero at the messenger scale safely. However, despite being negligibly small at $M_{\rm Mess}$, they can grow through RGEs easily up to about an order of TeV, and still be effective at the low scale observables. Similarly, the NH terms, in general, can be induced by the higher order operators effectively as [26,27]

$$\begin{aligned}
\frac{1}{M^3}\int d^4x d^4\theta \hat{X}\hat{\bar{X}}^\dagger \hat{\Phi}_i\hat{\Phi}_j\hat{\Phi}_k^\dagger &= \frac{\mathcal{F}^2}{M^3}S_iS_jS_k^* \to A' S_iS_jS_k^*,\\
\frac{1}{M^3}\int d^4x d^4\theta \hat{X}\hat{\bar{X}}^\dagger \mathcal{D}^\alpha\hat{\Phi}\mathcal{D}_\alpha\hat{\Phi} &= \frac{\mathcal{F}^2}{M^3}\psi\psi \to \mu'\psi\psi,
\end{aligned} \quad \text{(2.4)}$$

which can be adapted to the GMSB-ADJ models by setting $M \to M_{\rm Mess}$ and $\mathcal{F}^2 \to \sum_i \langle F_i\rangle^2$, and the typical order for the NH terms is found as

$$A', \mu' \sim \frac{1}{M_{\rm Mess}}\sum_i \Lambda_i^2. \quad \text{(2.5)}$$

In this context, the NH terms are suppressed by $1/M_{\rm Mess}$ as the holomorphic trilinear SSB couplings. However, it may not be a good approximation for the NH terms, since the RGEs do not have a growing effect on the NH terms unless one assumes another source which induces considerable NH interactions [46], as can be seen from the following RGEs:

$$\begin{aligned}
\frac{d\mu'}{dt} &= \frac{1}{16\pi^2}\left(y_\tau^2+3y_b^2+3y_t^2-3g_2^2+\frac{3}{5}g_1^2\right)\mu'\\
\frac{dA_t'}{dt} &= \frac{1}{16\pi^2}\left[\left(y_\tau^2+5y_b^2+3y_t^2\right)A_t'+2y_b^2\left(A_b'-2\mu'\right)\right.\\
&\quad \left.+\left(A_t'-2\mu'\right)\left(3g_2^2+\frac{3}{5}g_1^2\right)\right]\\
\frac{dA_b'}{dt} &= \frac{1}{16\pi^2}\left[\left(-y_\tau^2+3y_b^2+5y_t^2\right)A_b'+2y_t^2\left(A_t'-2\mu'\right)\right.\\
&\quad \left.+\left(A_b'-2\mu'\right)\left(3g_2^2+\frac{3}{5}g_1^2\right)\right]\\
\frac{dA_\tau'}{dt} &= \frac{1}{16\pi^2}\left[\left(y_\tau^2-3y_b^2+3y_t^2\right)A_\tau'+6y_b^2A_b'\right.\\
&\quad \left.+\left(A_\tau'-2\mu'\right)\left(3g_2^2+\frac{3}{5}g_1^2\right)\right]
\end{aligned} \quad \text{(2.6)}$$

As is seen from the RGEs given in Eq. (2.6), setting the NH terms to zero at $M_{\rm Mess}$ fixes them to zero at all the energies. Hence, we keep them small but non-zero in our analyses. The resultant SSB Lagrangian, then, can be summarized as follows:

$$\begin{aligned}
\mathcal{L}_{\rm soft}^{\rm MSSM} = &-\frac{1}{2}\left(M_1\tilde{B}\tilde{B}+M_2\tilde{W}\tilde{W}+M_3\tilde{g}\tilde{g}\right)\\
&-\left(\tilde{Q}^\dagger m_Q^2\tilde{Q}+\tilde{L}^\dagger m_L^2\tilde{L}+\tilde{\bar{u}}m_u^2\tilde{\bar{u}}^\dagger\right.\\
&\left.+\tilde{\bar{d}}m_d^2\tilde{\bar{d}}^\dagger+\tilde{\bar{e}}m_e^2\tilde{\bar{e}}^\dagger\right)\\
&-m_{H_u}^2H_u^\dagger H_u-m_{H_d}^2H_d^\dagger H_d\\
&-(A_u\bar{Q}H_uu+A_d\bar{Q}H_dd+A_e\bar{L}H_de)\\
&+(bH_dH_u+\text{c.c.})\\
&-\mu'\tilde{H}_u\cdot\tilde{H}_d-\tilde{Q}\,H_d^\dagger A_u'\tilde{U}-\tilde{Q}\,H_u^\dagger A_d'\tilde{D}\\
&-\tilde{L}\,H_u^\dagger A_e'\tilde{E}-\text{h.c.}
\end{aligned} \quad \text{(2.7)}$$

In the MSSM, the Higgs boson mass receives radiative contributions mainly from stops and their mixing, while those from sbottom and stau can provide minor improvements, especially in the moderate $\tan\beta$ region [7]. On the other hand, in the presence of the NH terms, such minor contributions can be enhanced slightly [35,36]. In addition, the NH terms impose direct couplings for sbottom and stau to H_u, and such terms allow these supersymmetric particles to contribute directly to the SM-like Higgs boson. Such contributions can diminish the impact from the Higgs boson analyses on the implications of BSM models.

2.1 NH contributions to SUSY spectra

The main radiative supersymmetric contributions to the Higgs boson mass arise from the self-energy diagrams in which the squarks and sleptons run in the loop. In this context, the mixing in the mass-square matrices of these supersymmetric particles plays a crucial role. The NH terms directly alter the mixing among these particles, and their effects can be understood best by considering the relevant mass-square matrices

$$m^2_{\tilde{f}} = \begin{pmatrix} m_{\tilde{f}_L \tilde{f}_L^*} & X_{\tilde{f}} \\ X^*_{\tilde{f}} & m_{\tilde{f}_R \tilde{f}_R^*} \end{pmatrix} \tag{2.8}$$

in the basis $(\tilde{f}_L, \tilde{f}_R)$ and $(\tilde{f}_L^*, \tilde{f}_R^*)$. The diagonal elements in the mass-square matrix remain the same as those in the MSSM [47], while the mixing terms are modified by the NH terms as follows:

$$X_{\tilde{t}} = -\frac{m_t}{\sqrt{2}}\left[(\mu + A'_t)\cot\beta - A_t\right], \tag{2.9-a}$$

$$X_{\tilde{b}} = -\frac{m_b}{\sqrt{2}}\left[(\mu + A'_b)\tan\beta - A_b\right], \tag{2.9-b}$$

$$X_{\tilde{\tau}} = -\frac{m_\tau}{\sqrt{2}}\left[(\mu + A'_\tau)\tan\beta + A_\tau\right]. \tag{2.9-c}$$

The contributions from the NH term associated with the stops (A'_t) are inversely proportional to $\tan\beta$, and hence, one can expect some minor contributions from A'_t to the Higgs boson mass. On the other hand, these terms appear together with $\tan\beta$ in the sbottom and stau mass-square matrices, thus their contributions to the Higgs boson mass are enhanced with $\tan\beta$. We should note about the stability of the scalar potential before concluding this discussion that the coupling of the Higgs boson to staus, in particular, may lead to instability [7,48].

Once the NH terms are taken into account effectively at the low scale, their contributions to the masses appear only in their mixing, as summarized above, while the diagonal elements remain intact in the mass-square matrices given in Eq. (2.3-b). On the other hand, if the NH terms are imposed at the SUSY breaking scale in the visible sector (M_{Mess} in GMSB models), and involved in the RGEs, then these diagonal terms receive some NH corrections, as well. The NH effects in these mass terms can be seen in the following RGEs:

$$\begin{aligned}
\frac{dm^2_{\tilde{t}_R}}{dt} &= \left(\frac{dm^2_{\tilde{t}_R}}{dt}\right)_{\text{MSSM}} + 4y_t^2(A_t'^2 - 2|\mu'|^2) \\
\frac{dm^2_{\tilde{b}_R}}{dt} &= \left(\frac{dm^2_{\tilde{b}_R}}{dt}\right)_{\text{MSSM}} + 4y_b^2(A_b'^2 - 2|\mu'|^2) \\
\frac{dm^2_{\tilde{t}_L}}{dt} &= \left(\frac{dm^2_{\tilde{t}_L}}{dt}\right)_{\text{MSSM}} + 2y_t^2 A_t'^2 + 2y_b^2 A_b'^2 \\
&\quad -4|\mu'|^2(y_t^2 + y_b^2) \\
\frac{dm^2_{\tilde{\tau}_R}}{dt} &= \left(\frac{dm^2_{\tilde{\tau}_R}}{dt}\right)_{\text{MSSM}} + 2y_\tau^2(A_\tau'^2 - 2|\mu'|^2) \\
\frac{dm^2_{\tilde{\tau}_L}}{dt} &= \left(\frac{dm^2_{\tilde{\tau}_L}}{dt}\right)_{\text{MSSM}} + 2y_\tau^2(A_\tau'^2 - 2|\mu'|^2)
\end{aligned} \tag{2.10}$$

In this context, the NH terms can alter the masses in the full basis, and they even change the decoupling scale for the SUSY particles. Among the RGEs given above, the NH contributions can be crucial especially for the right-handed stau mass. As seen from the mass-square relations given in Eq. (2.3-b), small Λ_5 values can lead to inconsistently light or even tachyonic states for the right-handed stau field [21,22]. However, in the presence of the NH terms, one can keep the right-handed stau mass-square in consistent ranges. In addition to stau masses, the NH contributions to the stop masses can indirectly spread the NH effects over the whole spectra, since they change the SUSY decoupling scale M_{SUSY}. In this context, even though there is no direct NH contributions in case of some particles, such as gauginos, the whole spectrum is affected indirectly by the NH terms.

2.2 NH contributions to the Higgs boson mass

As is a well-known fact, the SM-like Higgs boson mass in MSSM is strongly based on its interactions with the stop. Hence, the mixing and masses in the stop sector play the most crucial role. The radiative contributions to the SM-like Higgs boson mass can be written as [7]

$$\begin{aligned}
\Delta m_h^2 \simeq\ & \frac{m_t^4}{16\pi^2 v^2 \sin^2\beta}\frac{\mu A_t}{M^2_{\text{SUSY}}}\left[\frac{A_t^2}{M^2_{\text{SUSY}}} - 6\right] \\
& + \frac{y_b^4 v^2}{16\pi^2}\sin^2\beta\frac{\mu^3 A_b}{M^4_{\text{SUSY}}} + \frac{y_\tau^4 v^2}{48\pi^2}\sin^2\beta\frac{\mu^3 A_\tau}{m^4_{\tilde{\tau}}},
\end{aligned} \tag{2.11}$$

where the first line represents the dominant contributions from stops, while the second line displays the minor contributions from sbottom and stau. These contributions in MSSM are restricted further by the stability condition of the Higgs potential [7,48]. In the presence of the NH terms, the trilinear couplings in Eq. (2.11) should be replaced as $A_i \to X_{\tilde{i}}$, where $X_{\tilde{i}}$ are given in Eqs. (2.9-a, 2.9-b and 2.9-c) for $i = \tilde{t}, \tilde{b}, \tilde{\tau}$. respectively. With this inclusion of the NH terms, the contributions from stops are enhanced, but it is expected to be small due to the suppression by $\tan\beta$. Despite small NH effects in stops through their mixing, they can still be significant with their RGE effects on the stop masses. In addition, the NH terms induce a direct coupling between $\tilde{b}, \tilde{\tau}$ and H_u, and they contribute to the SM-like Higgs boson directly as stop (for a detailed analyses see, for instance, [35,40]).

3 Scanning procedure and experimental constraints

In this section, we will briefly summarize the fundamental parameter space of the models in the GMSB-ADJ class, which is supplemented with the NH terms. In our work, we do not assume any sources by SUSY breaking, and hence, their values can be calculated in terms of the fundamental parameters of the GMSB-ADJ models as given in Eq. (2.5) (for possible mechanisms inducing NH terms see, for

instance, [31,46,49,50]). The fundamental parameters and their ranges in our analyses can be summarized as follows:

$$\begin{aligned} 10^{-7} \leq \quad & \Lambda_{5,3,8} && \leq 10^{7} \ \text{GeV} \\ 10^{6} \leq \quad & M_{Mess} && \leq 10^{16} \ \text{GeV} \\ 1.2 \leq \quad & \tan\beta && \leq 60, \\ & \text{sgn}(A'), \text{sgn}(\mu') && = -1, +1. \end{aligned} \tag{3.1}$$

where $\Lambda_{5,3,8}$ and M_{Mess} are the SUSY breaking parameters as defined in the previous section. $\tan\beta$ is parametrized by VEVs of the MSSM Higgs fields as $\tan\beta \equiv v_u/v_d$, in which v_u and v_d are VEVs of H_u and H_d, respectively. Based on Eq. (2.5), the magnitude of the NH terms can lie from about 10^{-30} GeV up to about 200 TeV with these ranges of the fundamental parameters. We also should note that we parametrize the strength of the NH trilinear interactions as $T'_i \equiv A'_i y_i$. With this setup, we keep the CKM matrix in rotation of the squark mass-square matrices, and also the NH terms do not lead to charged lepton flavour violation. Even though the numerical values of the NH terms are fixed with Λ_i and M_{Mess}, we assign positive and negative signs to the NH terms randomly.

The data analyzed in our work were generated by using SPheno-4.0.4 [12,51], which was generated with SARAH [52,53]. We have modified the SARAH package such that the NH terms can be imposed at the messenger scale, and run down to M_{SUSY} through RGEs. We performed random scans over the fundamental parameters within their ranges given in Eq. (3.1), and we use the Metropolis-Hastings algorithm [54,55]. SPheno first runs the 1-loop RGEs for the Yukawa and gauge couplings from M_Z to M_{Mess}. Once the numerical values are determined at M_{Mess}, all the SSB parameters parametrized with Λ_i and M_{Mess} are imposed and SPheno evolves masses and couplings back to M_{SUSY} through the 2-loop RGEs, where $M_{\text{SUSY}} \equiv \sqrt{m_{\tilde{t}_L} m_{\tilde{t}_R}}$ is the scale at which the supersymmetric particles decouple from the spectrum. The results from SPheno runs include the masses of the supersymmetric particles and Higgs bosons, couplings as well as the branching ratios for the on-shell decay processes.

After the data set is generated, we apply some experimental constraints successively from the mass bounds on the supersymmetric particles [56–59] and the Higgs boson [1–3], rare decays of B-meson [60,61], and the precision parameters [11]. These constraints can be summarized as follows:

$$\begin{aligned} & & m_{\tilde{g}} & && \geq 2.2 \ \text{TeV} & \\ 123 \leq & & m_h & && \leq 127 \ \text{GeV} & \\ 2.9 \times 10^{-4} \leq & & BR(b \to s\gamma) & && \leq 3.87 \times 10^{-4} & (2\sigma) \\ 1.95 \times 10^{-9} \leq & & BR(B_s \to \mu^+\mu^-) & && \leq 3.43 \times 10^{-9} & (2\sigma) \\ -0.14 \leq & & S & && \leq 0.06 & (1\sigma) \\ -0.11 \leq & & T & && \leq 0.13 & (1\sigma) \\ -0.1 \leq & & U & && \leq 0.08 & (1\sigma) \end{aligned} \tag{3.2}$$

One of the challenges in numerical data is the precision of the Higgs boson mass calculation. Despite precise experimental analyses, the theoretical uncertainties can exceed about 2 GeV arising from the uncertainties in top quark mass and strong couplings, as well as mixing among the sfermions [62–68]. Different techniques have been developed to improve the theoretical calculations of the Higgs boson mass such as considering higher order corrections, resummation large logarithms etc [14,69–72]. The impact from these corrections can be as high as about a 3 GeV difference in the Higgs boson mass [15] for large mixing in the sfermions, while it can be realized at about $0.5 - 1$ GeV when the mixing is relatively small [16] (A_0, $A'_0 \lesssim m_0$ as it happens in GMSB models).

The constraints from rare B-meson decays represent results from very sensitive experimental analyses and they constrain the BSM models almost in a model independent way. In addition, they provide a strong control on the heavy Higgs bosons as well. The new physics contributions to the $B_s \to \mu\mu$ are provided by the CP-odd and CP-even Higgs bosons [73,74], and the sensitive experimental analyses provide a fit on the coupling between these Higgs bosons and the charged SM leptons especially when they weigh about a TeV. Similarly, the charged Higgs boson can enhance the quark lepton flavor violation (QFV) and can be constrained by the results from $b \to s\gamma$ analyses, which provide a fit on their couplings to the quarks. After imposing these constraints we did not expect a significant impact from the numerical packages which are specialized on the Higgs bosons. However, they do not guarantee to be compatible with the Higgs boson results for every single solution. Therefore, we transferred our data to the HiggsBounds and HiggsSignals [75], before presenting our results. A recent update on the precision parameters (S, T, U) [76] are also considered relevant and we include their current bounds within 1σ [11] in the constraint set employed in our analyses as listed in Eq. (3.2). These parameters can imply some deviations in the mass of W-boson [77]. The current measurements from the CDF experiment [78] imply a large deviation in M_W; however, it requires inconsistently light Higgs bosons within the MSSM framework, and such solutions are more likely excluded by the rare B-meson decays. In our analyses we set it to the SM value as $M_W = 80.357$ GeV, which is also compatible with the current CMS measurements [79].

In addition to these constraints, we also accept only the solutions which are compatible with the radiative electroweak symmetry breaking (REWSB). This condition imposes tadpole equations for μ and b terms as follows:

$$\begin{aligned} m^2_{H_u} + |\mu|^2 - b\cot\beta - \frac{1}{2}M_Z^2\cos(2\beta) = 0 \\ m^2_{H_d} + |\mu|^2 - b\tan\beta + \frac{1}{2}M_Z^2\cos(2\beta) = 0 \end{aligned} \tag{3.3}$$

Since the fundamental parameters of our model determine square of the SSB masses of H_u and H_d, we impose $m^2_{H_u}$ and $m^2_{H_d}$, and calculate μ and b through these tadpole equations regardless to their high scale origin. However it does not mean that the NH contributions are not taken into account for these terms. These contributions are involved in calculation of $m^2_{H_u}$ and $m^2_{H_d}$, and they can affect the consistent values for μ and b terms. Note that, despite its certain value, the sign of μ remains undetermined, so it can be treated as to be one of the free parameters. In our scans, however, we set its sign to be positive for every solution. Finally, after the recent updates in muon $g-2$, we also require our solutions do not spoil the muon $g-2$ results with large or negative SUSY contributions by imposing the constraint as $0 \leq \Delta a_\mu \leq 6.6 \times 10^{-10}$ [80,81].

As is well known the GMSB models usually yield gravitino to be the lightest supersymmetric particle (LSP) in the spectrum. However, the models in the GMSB-ADJ class can also lead to MSSM neutralinos to be LSP in a small portion of their fundamental parameter space [21]. These two different cases of LSP lead to different phenomenology, and hence, they might be subjected to different experimental results, when they are considered to be candidates of dark matter (DM). Considering the possible NH contributions in the DM phenomenology, we accept only the solutions which accommodate either gravitino or one of the MSSM neutralinos to be LSP in the spectrum. However, despite including in our analyses, we do not observe any significant effect from the NH contributions in the DM implications of the models; and hence, we leave it out of the scope of our work.

4 Fundamental parameter space of GMSB-ADJ

We first display the allowed ranges for the fundamental parameters $M_{\rm Mess}$ and Λ_5 in Fig. 1. All the points are compatible with the REWSB and condition on LSP to be either Gravitino or Neutralino. Green points are compatible with the constraints listed in Eq. (3.2). The left planes depict the results for the case in which the NH terms are absent, while the right planes are generated for the models including the NH contributions. Note that these two data sets are generated independently. As seen from the the $M_{\rm Mess}-\Lambda_5$ plane for the holomorphic case (top-left), Λ_5 cannot be smaller than about 10^3 GeV, and the solutions consistent with the experimental constraints employed in our analyses can be realized when $\Lambda_5 \gtrsim 2\times 10^5$ GeV, while $M_{\rm Mess}$ can lie in a wide range from 10^6 to 10^{16} GeV. This bound on Λ_5 arises from the stau mass. As discussed before, the right-handed stau mass is induced only through the interactions with Σ_5, and its SSB mass depends only on Λ_5. Therefore, small ranges of Λ_5 yield tachyonic states for the right-handed stau when $\Lambda_5 \lesssim 10^3$ GeV. Besides, despite avoiding the tachyonic states, stau happens inconsistently light for $10^3 \lesssim \Lambda_5 \lesssim 10^5$ GeV. These results can be seen in the $m_{\tilde\tau_1}-\Lambda_5$ plane for the holomorphic case (bottom-left).

The right planes show the results in the same planes for the solutions in which the NH contributions are also taken into account. The impact from such contributions can be directly seen in the regions with small Λ_5. As seen from the top-right $M_{\rm Mess}-\Lambda_5$, one can find solutions even in the regions with $\Lambda_5 \gtrsim 10^{-7}$ GeV. Clearly, the NH contributions in this region are large enough that the right-handed stau mass-square remains positive. However, the experimental mass bound on stau restricts $M_{\rm Mess}$ to be larger than about 10^8 GeV. We also observe an upper bound on $M_{\rm Mess}$ in this region as $M_{\rm Mess} \lesssim 10^9$ GeV. Above this region there is no solution at all, because the right-handed stau mass turns to be tachyonic again. Indeed, larger $M_{\rm Mess}$ means also RGE evolution in a larger energy interval. In this region, the Bino mass (M_1) also turns to be negative, and it starts reducing the stau mass through RGEs. A longer RG evolution leads M_1 to enhance its decreasing effect on the stau mass. In this case, although stau mass-square starts from positive, it falls into the negative values through its RG evolution when $M_{\rm Mess} \gtrsim 10^9$ GeV. We also display the stau mass in the parameter space in the bottom-right plane, which shows that the stau can be as heavy as about 15 TeV in this region.

The results shown in Fig. 1 in comparison with the holomorphic case reveal the significant impact from the NH terms. In the small Λ_5 region, following Eq. (2.5), at least one of the messenger fields should be heavy to induce relatively large NH terms. This requirement can be seen from the planes of Fig. 2, whose color coding is the same as in Fig. 1. The top planes display the ranges of Λ_3 (left) and Λ_8 (right) in comparison with Λ_5. As seen from the results in these planes, both Λ_3 and Λ_8 should be larger than about 10^4 in the regions with small Λ_5 to avoid tachyonic stau states. The consistent solutions (green) shift the scales for these parameters further to about 10^5 GeV. The order of the NH terms also inversely depends on $M_{\rm Mess}$, which requires relatively small values for the SUSY breaking scale. The $M_{\rm Mess}-A'_0$ plane shows that $M_{\rm Mess}$ cannot be larger than about 10^{11} GeV in order to induce sizeable NH terms. The solutions in this plane show that A'_0 can be as large as about 200 TeV. The $\Lambda_5 - A'_0$ plane shows that the stau is still realized inconsistently light in the region with $-10 \lesssim A'_0 \lesssim 20$ TeV. As also is seen, heavy stau masses mostly require negative A'_0, and heavy staus ($\sim$ 15 TeV) can be realized when $A'_0 \sim -200$ TeV.

4.1 Supersymmetric mass spectra

In this section, we discuss the NH contributions to the SUSY spectra by comparing the masses of SUSY particles with and

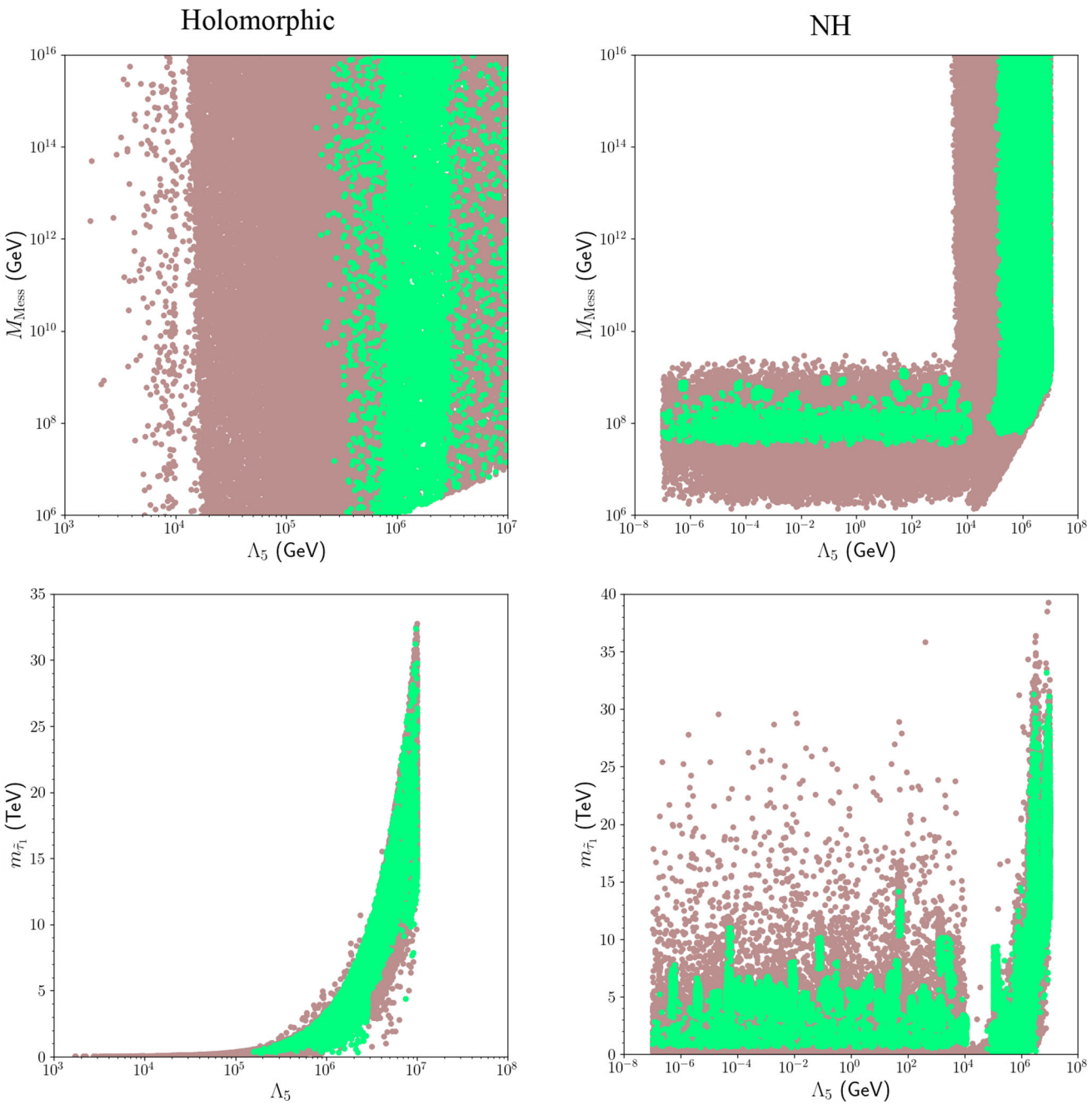

Fig. 1 The allowed ranges of the fundamental parameters $M_{\rm Mess}$ and Λ_5 in the absence of NH terms (left) and with the NH contributions (right). The bottom planes display the results for the stau mass, which is crucial to shape the ranges of Λ_5. All the points are compatible with the REWSB and condition on LSP to be either gravitino or neutralino. Green points are compatible with the constraints listed in Eq. (3.2)

without the NH terms. The solutions represented in this section are calculated twice one of which employs the NH terms, while the other set them to zero for the same input values (we call it the holomorphic case). Note that these results depict the solutions which do not lead to tachyonic states when the NH contributions are switched off, therefore the regions with $\Lambda_5 \lesssim 10^3$ GeV are not represented in these planes. The parameters calculated without the NH contributions are denoted with the upper index "H".

We discussed the crucial role of the stau mass in the previous section, so it might be better to show first the NH contributions to the right-handed stau mass. Figure 3 displays our results for the comparison in stau mass between the holomorphic and NH cases in the $m_{\tilde{\tau}_R} - m^H_{\tilde{\tau}_R}$ and $\Delta m_{\tilde{\tau}_R} - A'_0$

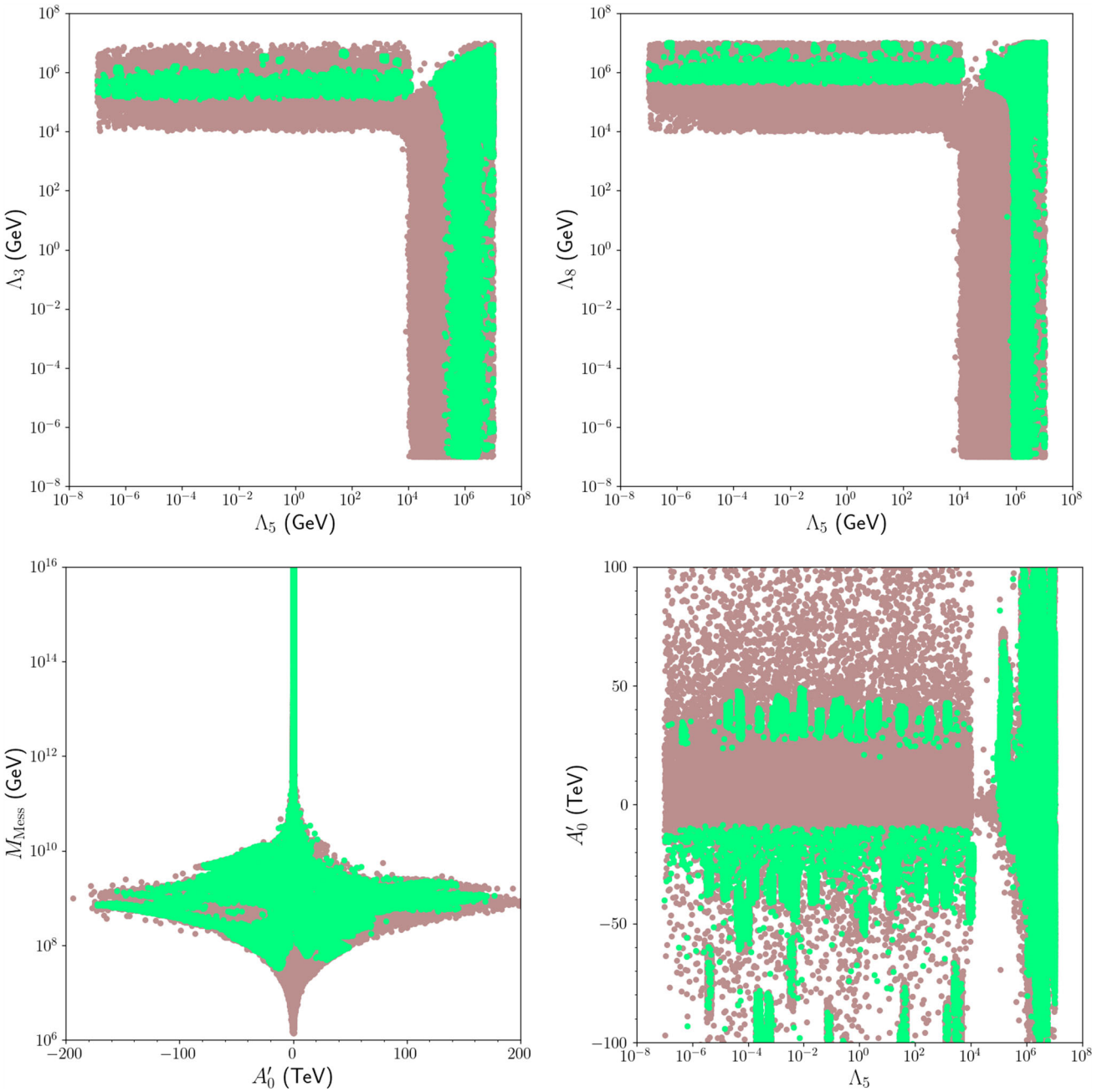

Fig. 2 Plots in the $\Lambda_3 - \Lambda_5$, $\Lambda_3 - \Lambda_8$, $M_{\rm Mess} - A_0'$, and $\Lambda_5 - A_0'$ planes. The color coding is the same as in Fig. 1

planes, where $\Delta m_{\tilde{\tau}_R} = m_{\tilde{\tau}_R} - m^H_{\tilde{\tau}_R}$. The color coding is the same as in Fig. 2. The diagonal line in the left plane depicts the solutions for negligible or zero NH contributions to the stau mass ($m_{\tilde{\tau}_R} = m^H_{\tilde{\tau}_R}$). As is seen, the light stau solutions in the holomorphic case (say $m^H_{\tilde{\tau}_R} \lesssim 1$ TeV) can be as heavy as about 10 TeV after the NH contributions are added. Besides, the stau can be as heavy as about 30 TeV with the NH contributions, while $m^H_{\tilde{\tau}_R} \lesssim 20$ TeV. The NH contributions become negligible in the regions when the holomorphic case involves staus heavier than about 20 TeV in the spectra, as observed that all the solutions are accumulated around the diagonal line when $m^H_{\tilde{\tau}_R} \gtrsim 20$ TeV. The correlation in the NH contributions to the stau mass with the NH terms is shown in the $\Delta m_{\tilde{\tau}_R} - A_0'$. As expected, the large A_0' values contribute most such that one can realize about 25 TeV difference in the stau mass when $|A_0'| \gtrsim 100$ TeV. Even though it seems the NH terms always contribute to the stau mass positively, there is a small region where they reduce the stau mass. However the difference in these solutions does not exceed 1 TeV so that it is not very visible in Fig. 3.

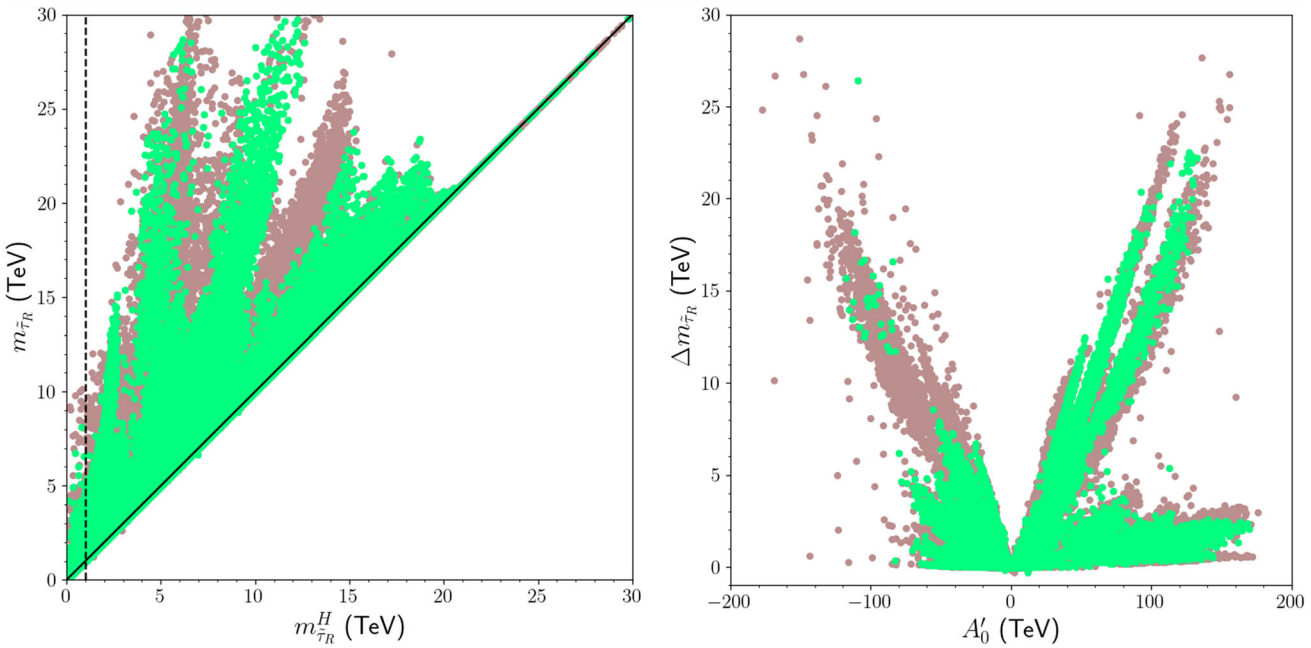

Fig. 3 The right-handed stau masses in holomorphic ($m^H_{\tilde{\tau}_R}$) and NH cases (left), the difference in its mass due to the NH contributions in correlation with its mixing (right). The color coding is the same as in Fig. 2. The diagonal line in the left plane depicts the solutions for negligible or zero NH contributions to the stau mass ($m_{\tilde{\tau}_R} = m^H_{\tilde{\tau}_R}$). The dashed vertical line is also used to indicate the solutions which lead to light staus in the holomorphic case ($m_{\tilde{\tau}_R} \leq 1$ TeV)

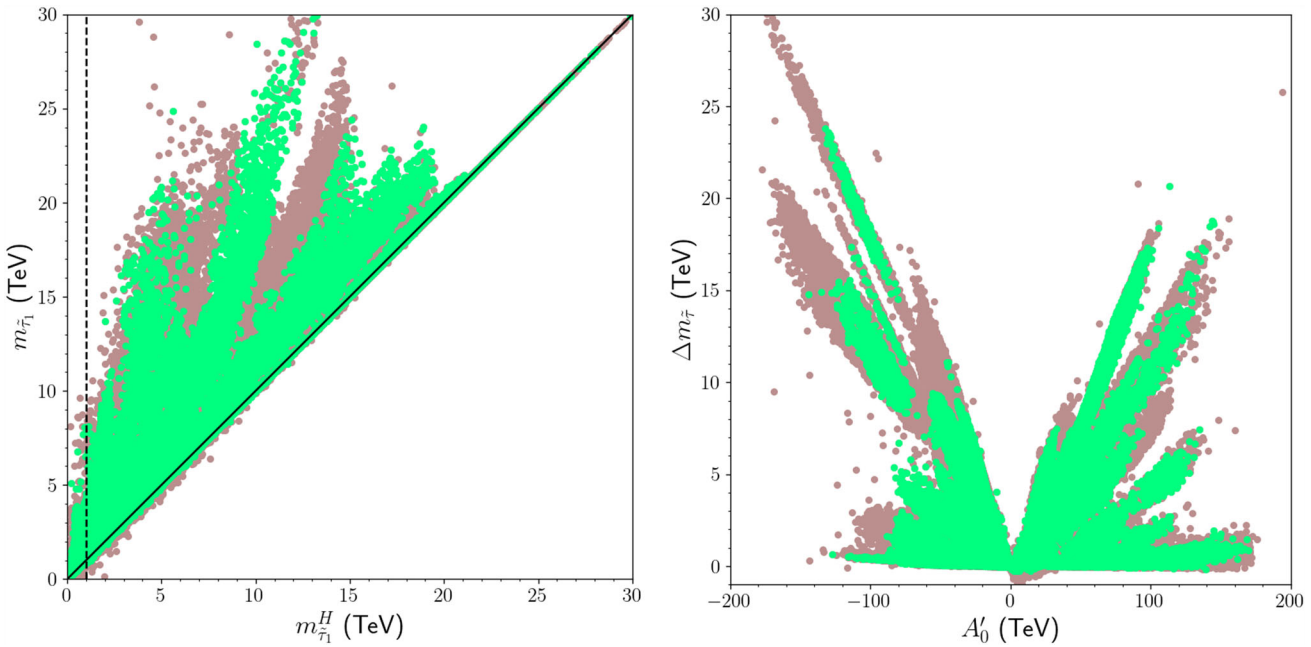

Fig. 4 Plots in the $m_{\tilde{\tau}_1} - m^H_{\tilde{\tau}_1}$ and $\Delta m_{\tilde{\tau}_1} - A'_0$ planes. The color coding is the same as in Fig. 1. The diagonal lines in each plane depict the solutions in which the NH contributions are negligible

Note that the right-handed staus receive the NH contributions only through RGEs. On the other hand, the mass eigenstates also receive these contributions through the mixing in their mass-square matrix as given in Eq. (2.8). Figure 4 represents the masses for the lightest stau mass eigenstate in comparison with the holomorphic case in the $m_{\tilde{\tau}_1} - m^H_{\tilde{\tau}_1}$ plane, and the NH contributions in the $\Delta m_{\tilde{\tau}_1} - A'_0$ plane. The color coding is the same as in Fig. 1. The diagonal lines in the

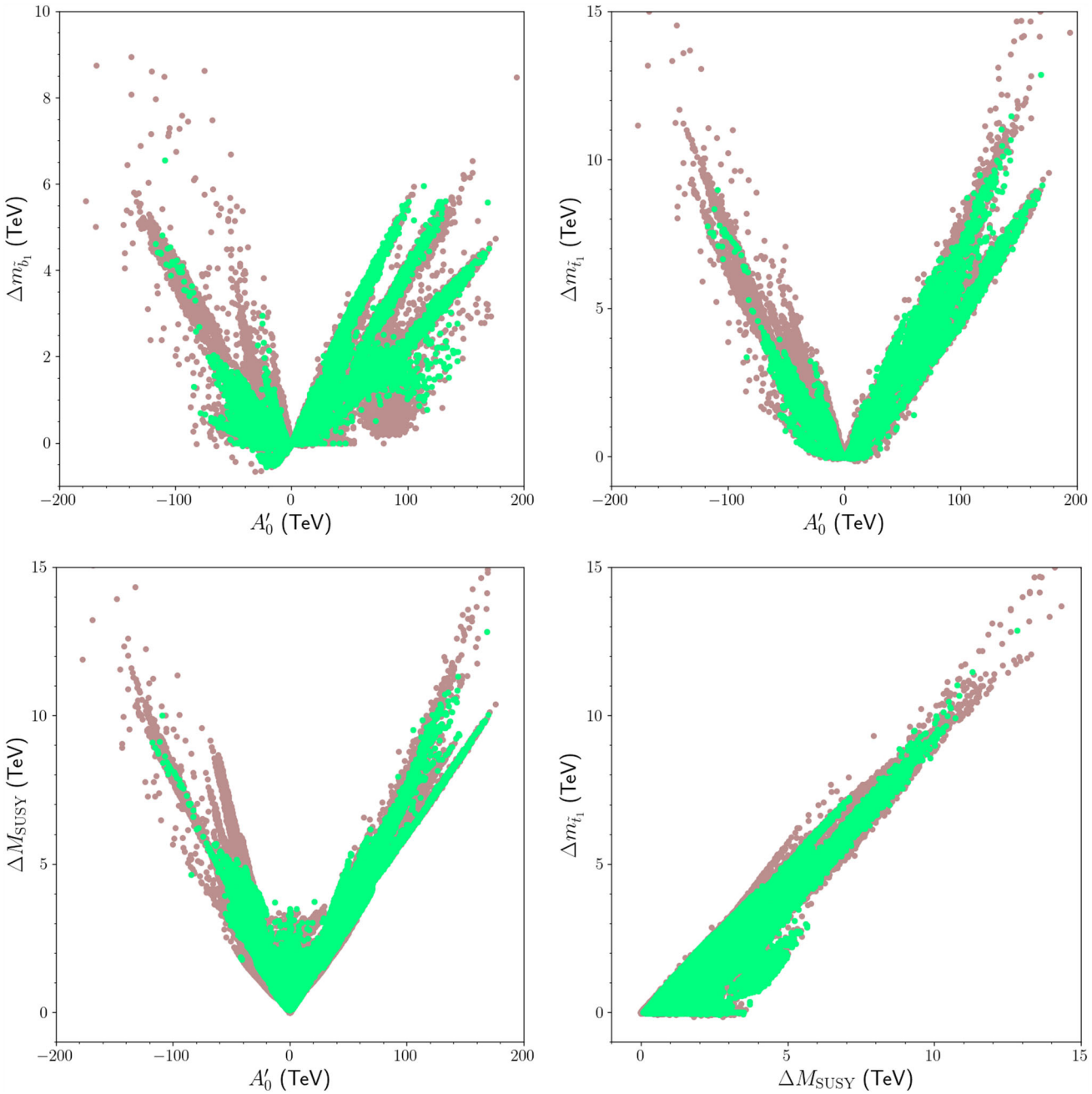

Fig. 5 The NH contributions to the squarks in the $\Delta m_{\tilde{b}_1} - A'_0$, $\Delta m_{\tilde{t}_1} - A'_0$, $\Delta M_{\rm SUSY} - A'_0$, and $\Delta m_{\tilde{t}_1} - \Delta M_{\rm SUSY}$ planes. The color coding is the same as in Fig. 1

left plane depicts the solutions in which the NH contributions are negligible. The solutions in the $m_{\tilde{\tau}_1} - m^H_{\tilde{\tau}_1}$ shows a similar behaviour as mass of the flavour eigenstate $m_{\tilde{\tau}_R}$. On the other hand, we observe that the difference from the holomorphic case is slightly smaller for the mass eigenstates. The heaviest stau mass can be realized at about 30 TeV, which corresponds to about 20 TeV mass difference from the holomorphic case at most. The solutions which yield light staus ($m^H_{\tilde{\tau}_1} \lesssim 1$ TeV) in the holomorphic case, can accommodate staus as heavy as about 7–8 TeV with the NH contributions. The correlations with the mass difference and the NH terms can be seen in the $\Delta m_{\tilde{\tau}_1} - A'_0$ plane, and it is quite similar to that observed in the $\Delta m_{\tilde{\tau}_R} - A'_0$ plane.

We conclude the NH contributions to the SUSY spectra by investigating their effects on the squark masses in Fig. 5 with the $\Delta m_{\tilde{b}_1} - A'_0$, $\Delta m_{\tilde{t}_1} - A'_0$, $\Delta M_{\rm SUSY} - A'_0$, and $\Delta m_{\tilde{t}_1} - \Delta M_{\rm SUSY}$ planes. The color coding is the same as in Fig. 1. Even though one expects a similar effect on the sbot-

tom mass, the $\Delta m_{\tilde{b}_1} - A'_0$ plane reveals smaller changes in the sbottom mass due to the NH contributions. It is because the large Λ_8 values, which is required by the heavy mass bounds on the squarks and gluinos from the experimental analyses. As we concluded from results in the $m_{\tilde{\tau}_R} - m^H_{\tilde{\tau}_R}$ plane that the NH contributions become negligible in the heavy mass spectra. Large Λ_8 values lead to heavy sbottoms and the NH contributions are as large as only about 7 TeV. On the other hand, an interesting result can be observed in the $\Delta m_{\tilde{t}_1} - A'_0$ plane that the stop mass can differ by about 13–14 TeV. The NH effects through mixing in stop sector are suppressed by $\tan\beta$, so we do not observe a strong reducing effect from the NH contributions in their mixing. On the other hand, the difference in the stop mass modifies the renormalization scale in a way that heavy stops lead to SUSY particles decoupling from the spectra at higher energy scales. A similar difference by 13–14 TeV is also realized in $M_{\rm SUSY}$ as shown in $\Delta M_{\rm SUSY} - A'_0$ plane. In this case, the SUSY particles decouple from the spectra at their heavier mass scales. The modification in the renormalization scale indirectly affects all the mass spectrum. The $\Delta m_{\tilde{t}_1} - \Delta M_{\rm SUSY}$ plane reveals a nearly linear correlation between $\Delta m_{\tilde{t}_1}$ and $\Delta M_{\rm SUSY}$.

4.2 NH contributions to the Higgs boson mass

In the previous section, we observed mostly positive contributions from the NH terms to sfermions, though negative contributions can also be realized in a small region. In contrast to the positive contributions, however, the negative contributions do not exceed about 1 TeV. On the other hand, the SM-like Higgs boson mass might exhibit a significant sensitivity to the positive and negative NH contributions. We present our results for the SM-like Higgs boson in Fig. 6 in comparison with the holomorphic case and the correlation between the NH contributions and mixing in sfermions. The color coding is the same as in Fig. 1. The experimental bound on the Higgs boson mass is not applied in the $m_h - m^H_h$ plane, but these bounds are rather represented by the horizontal and vertical dashed lines in this plane. The diagonal line in the top-left plane and the horizontal dashed lines in the other planes depict the solutions with negligible NH contributions. The overall mass difference in the SM-like Higgs boson can be realized as large as about 80 GeV in both cases of negative and positive NH contributions. The $m_h - m^H_h$ plane shows that especially large positive contributions can bring the SM-like Higgs boson mass to the experimentally consistent scales (green in between two horizontal dashed lines), even if it weighs about 40 GeV in the holomorphic case. However, the large negative contributions can happen when the both NH and holomorphic cases yield inconsistently light SM-like Higgs boson. The results in the $\Delta m_h - \Delta(X_\tau/M_{\rm SUSY})$ plane reveal that the large positive contributions arise from the NH contributions to the ratio $X_\tau/M_{\rm SUSY}$ such that large values for this ratio lead to large positive contributions to the Higgs boson mass. On the other hand, when the contributions to this ratio are small and/or negative, the NH contributions lower the SM-like Higgs boson mass compared to the results in the holomorphic case. In the experimentally consistent region (green), the largest negative contribution to the SM-like Higgs boson mass is observed at about 20 GeV. Although it is not as large as those from the stau mixing, the sbottom mixing also minorly contributes to the Higgs boson mass. These solutions happen in the region with $X_t/M_{\rm SUSY} \sim 0$; however it can help driving positive contributions to the Higgs boson mass when $\Delta(X_t/M_{\rm SUSY}) \sim -0.3$, as seen from the $\Delta m_h - \Delta(X_t/M_{\rm SUSY})$.

Before concluding the SM-like Higgs boson discussions, one should also consider the implications and the impacts from the NH terms in the heavy Higgs boson searches. Indeed, the Higgs bosons exhibit similar features to those obtained in MSSM analyses without the NH terms such as the mass degeneracy at the decoupling limit, contributions to rare B-meson decays listed among the constraints in Eq. (3.2) etc. We have presented the masses of the heavy Higgses and the NH contributions in their masses in Fig. 7. The color coding is the same as in Fig. 1. As is seen from the $m_A - m_H$, the mass degeneracy still holds after the NH contributions are considered. Indeed, it is expected when the SSB Higgs masses are quite heavy at the high scale. In these cases, the SM-like Higgs boson is formed almost purely by H_u because of its direct couplings to top quark and its superpartner stop. The other Higgs bosons are, consequently, formed by H_d. Such a composition in the Higgs sector also separate the NH contributions such that the NH couplings of the sbottom and stau to H_u contribute to the SM-like Higgs boson mass, while the NH coupling of stop to H_d is effective in the spectrum of the heavy Higgs bosons, We observe about -20 TeV difference in the Higgs boson masses when $A'_0 < 0$. The NH contributions can be as large as about -40 TeV in the region with $A'_0 > 0$.

Realizing relatively light Higgs boson masses with the NH contributions can lead to interesting implications in the direct Higgs boson searches. Figure 8 display the cross-section in correlation with the Higgs boson masses through the gluon fusion at 14 TeV. The color coding is the same as in Fig. 1. The blue and red curves display the current results from the experimental analyses performed by the CMS [82] and ATLAS [83] collaborations, respectively. The left panel represents the results for the cross-section in correlation with the CP-odd Higgs boson mass for the holomorphic case ($NH = 0$), while the right panel shows the same correlation when the NH terms are present. Note that since the heavy Higgs bosons are degenerate in mass, m_A represents also the other Higgs boson masses, and the cross-section is calculated by summing over all the $\tau\tau$ events involving the CP-odd or CP-even Higgs bosons ($\phi \equiv H, A$). As is seen from the left

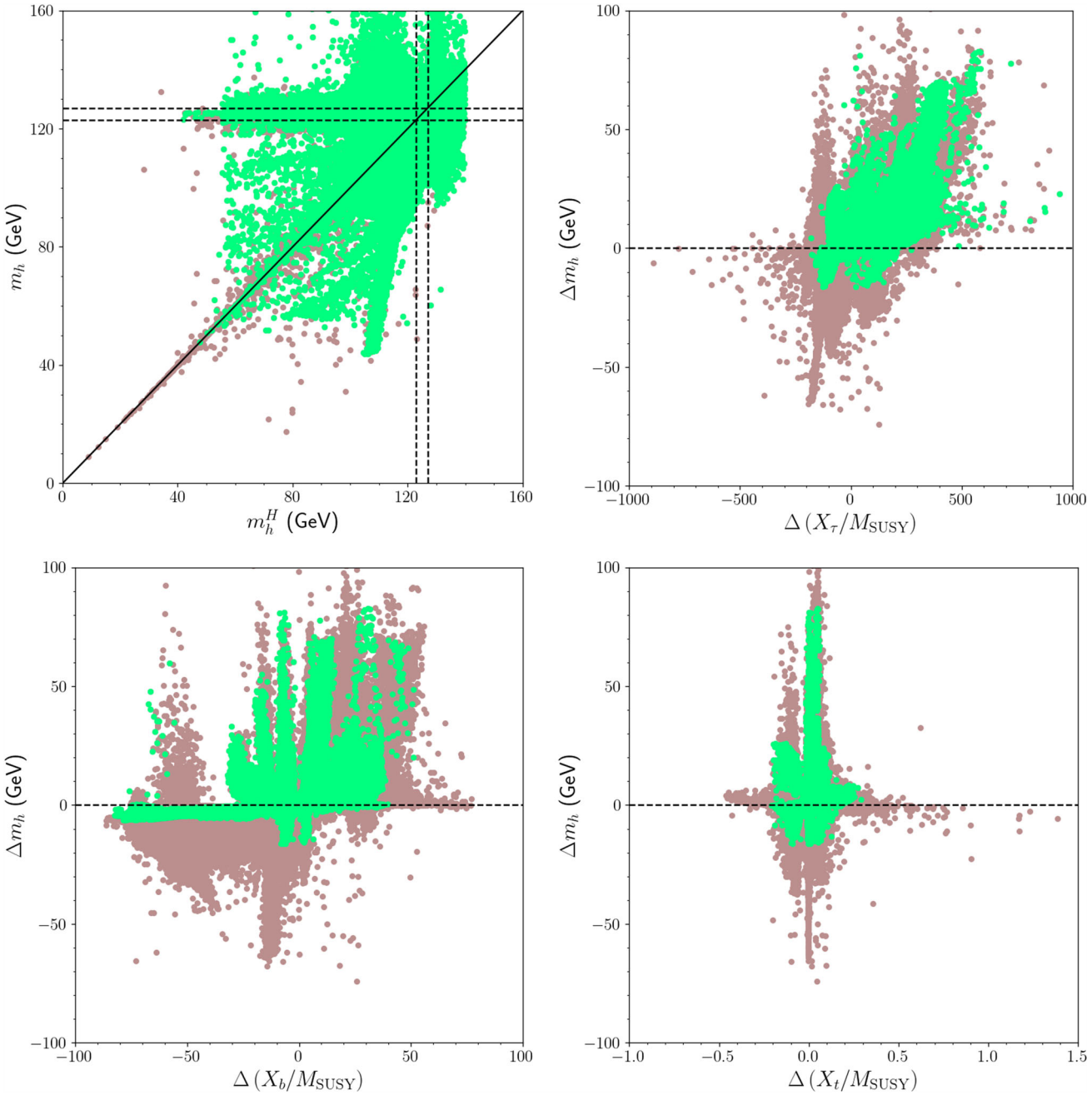

Fig. 6 The Higgs boson mass in comparison with the holomorphic case and the correlation between the NH contributions and mixing in sfermions. The color coding is the same as in Fig. 1. The experimental bounds on the Higgs boson mass is not applied in the $m_h - m_h^H$ plane, but these bounds are rather represented by the horizontal and vertical dashed lines in this plane. The diagonal line in the top-left plane and the horizontal dashed lines in the other planes depict the solutions with negligible NH contributions

panel, these Higgs bosons cannot be lighter than about 2 TeV (green points) without NH contributions and they lead to low cross-section results ($\lesssim 10^{-6}$ pb). The lighter Higgs boson solutions ($m_A < 2$ TeV) can yield large cross-sections, but these solutions are excluded due to inconsistently light SM-like Higgs boson. On the other hand, the NH contributions, as displayed in the right panel, can accommodate such Higgs bosons in the spectrum at about 1 TeV and they can imply large enough cross-sections ($\sim 10^{-2}$ pb) which are expected to be tested soon in the heavy Higgs boson searches. In these regions, the NH terms A'_b and A'_τ drive the SM-like Higgs boson to the heavier mass scales as discussed in Fig. 6, while A'_t lowers the masses of the heavy Higgs bosons.

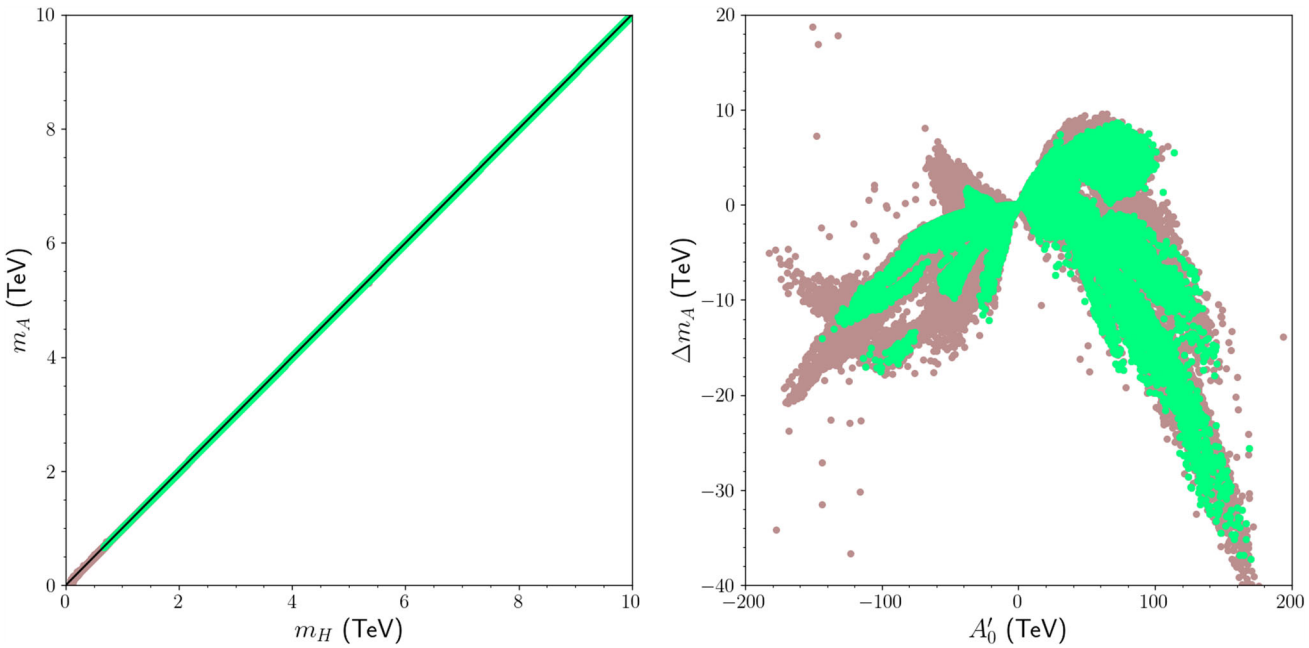

Fig. 7 The masses of the heavy Higgs bosons in $m_A - m_H$ plane (left) and the NH contributions in their masses in correlation with A_0' (right). The color coding is the same as in Fig. 1

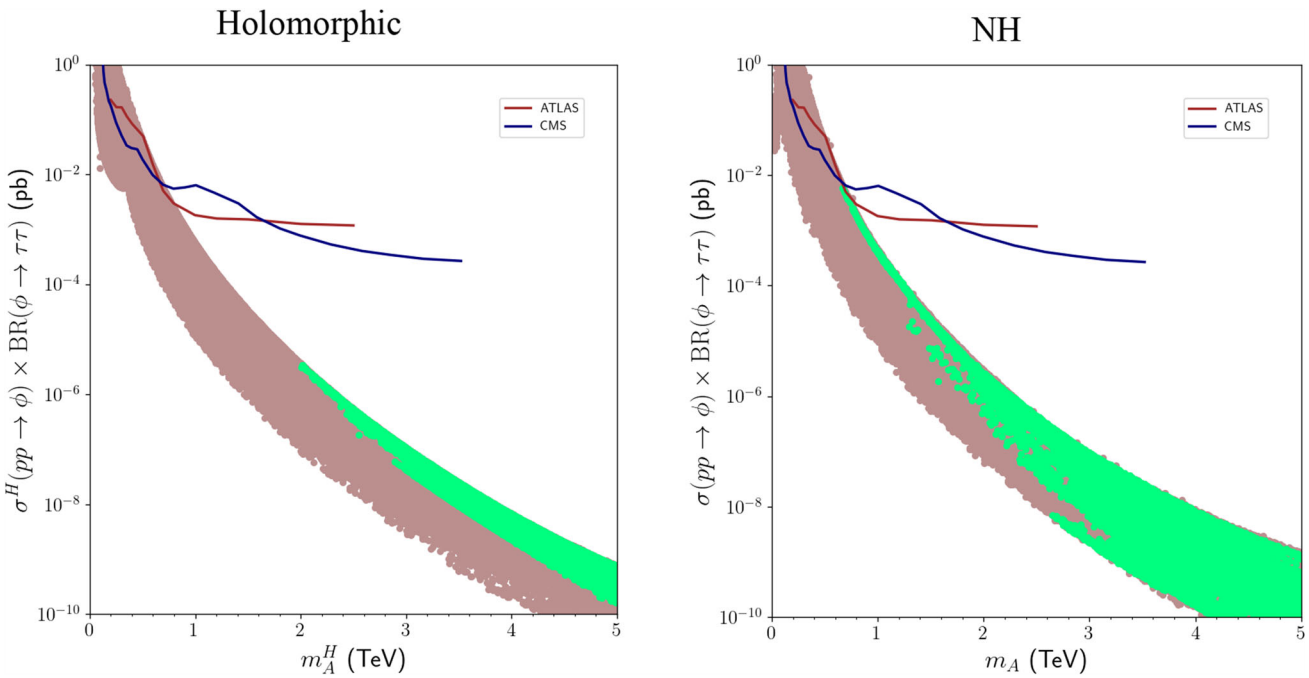

Fig. 8 The cross-section for the $A, H \to \tau\tau$ events through the gluon fusion at 14 TeV and the impacts from the NH terms. The color coding is the same as in figures represented in the manuscript. The blue and red curves in the top planes display the current results from the experimental analyses performed by the CMS [82] and ATLAS [83] collaborations, respectively. The left panel represents the results for the cross-section in correlation with the CP-odd Higgs boson for the holomorphic case ($NH = 0$), while the right panel represents the same correlation when the NH terms are present

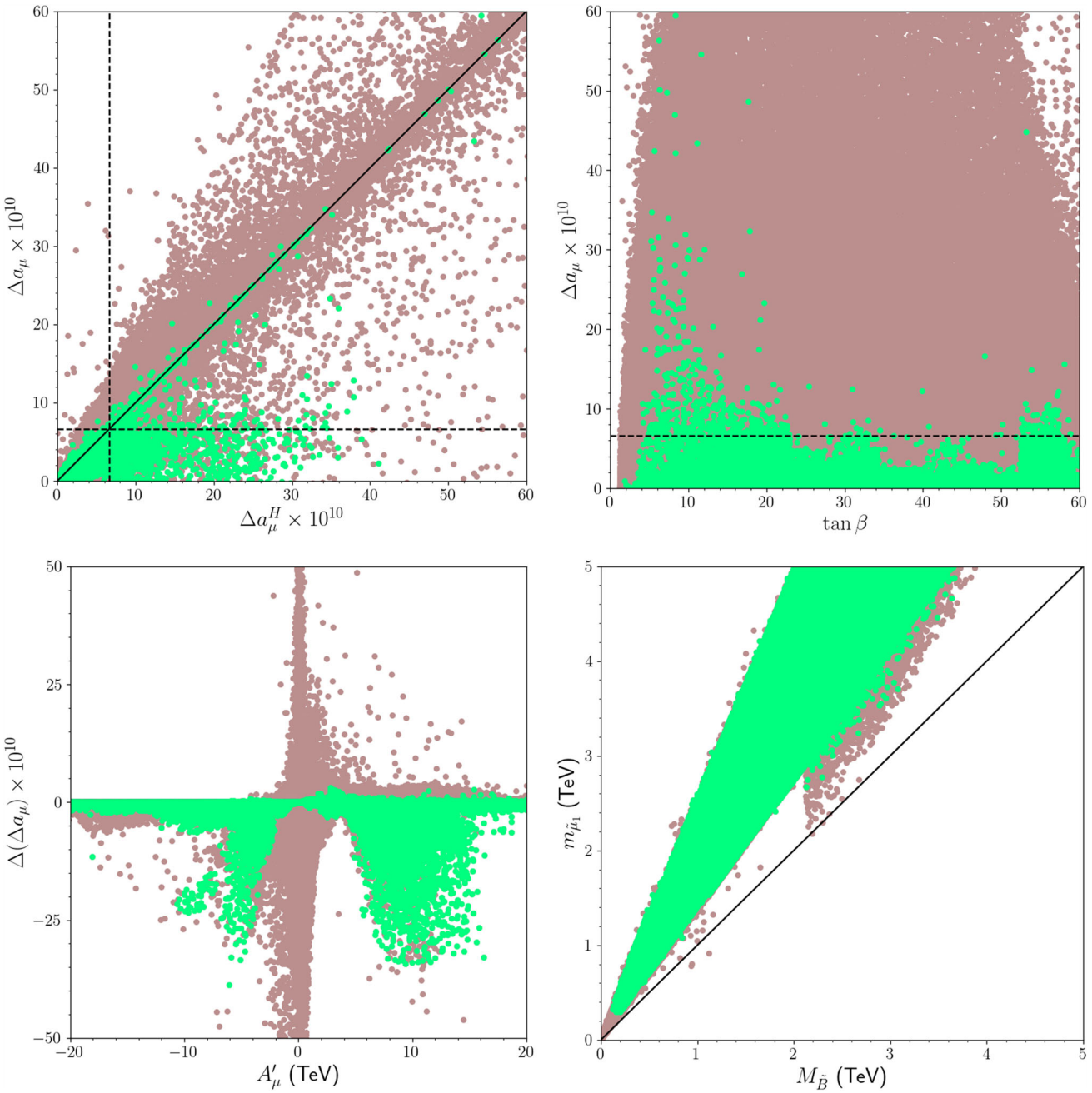

Fig. 9 The results for the muon anomalous magnetic moment and the NH contributions to it in the $\Delta a_\mu - \Delta a_\mu^H$, $\Delta a_\mu - \tan\beta$, $\Delta(\Delta a_\mu) - A'_\mu$, and $m_{\tilde{\mu}_1} - M_{\tilde{B}}$ planes. The color coding is the same as Figure 1. The horizontal and vertical dashed lines indicate the bound $\Delta a_\mu \leq 6.6 \times 10^{10}$ as recently reported by the White Paper (WP25) [80]. The horizontal line in the $\Delta a_\mu - \Delta a_\mu^H$ plane represents the solutions with negligible NH contributions to Δa_μ ($\Delta a_\mu = \Delta a_\mu^H$). Also, the diagonal line in the $m_{\tilde{\mu}_1} - M_{\tilde{B}}$ plane indicates the mass degeneracy between smuon and Bino ($m_{\tilde{\mu}_1} = M_{\tilde{B}}$)

Table 1 Benchmark points exemplifying our findings. All points are selected to be consistent with the experimental constraints employed in our analyses. All the points are selected by requiring to be consistent with the experimental constraints employed in our analyses. All the parameters, except Δa_μ, are expressed in units of GeV. The bold emphasize the parameters relevant to our discussions, while the italics shows the cases with negligible NH contributions

	Point 1	Point 2	Point 3	Point 4	Point 5
Λ_5	4.75×10^5	2.13×10^6	2.03×10^6	7.44×10^6	1.59×10^5
Λ_3	8.05×10^5	4.89×10^5	2.83×10^4	4.87×10^3	2.57×10^5
Λ_8	1.31×10^6	2.45×10^6	5.39×10^6	1.45×10^4	6.86×10^5
M_{Mess}	2.73×10^8	6.68×10^9	1.66×10^9	7.02×10^8	8.17×10^7
$\tan\beta$	55.6	51.4	47.0	59.9	14.1
A'_0, μ'	2.47×10^4	3.85×10^3	-3.34×10^4	7.93×10^4	1.49×10^4
A'_τ	1.65×10^4	2.27×10^3	-2.19×10^4	7.45×10^4	1.05×10^4
A'_b	1.18×10^4	1.44×10^3	-1.57×10^4	7.45×10^4	7.68×10^3
A'_t	1.49×10^4	1.88×10^3	-1.90×10^4	7.45×10^4	1.04×10^4
$m_{\tilde{\tau}_1}$, $\Delta m_{\tilde{\tau}_1}$	**5994**, **5931**	**3590**, **− 274.8**	10,131, 6446	23,869, 13,880	1027, 772.3
$m_{\tilde{b}_1}$, $\Delta m_{\tilde{b}_1}$	22,152, 1192	41,871, *20.5*	78,885, 905.3	53,906, 4566	11,917, 448.4
$m_{\tilde{t}_1}$, $\Delta m_{\tilde{t}_1}$	22,088, 1915	40,082, *-23.2*	77,200, 1561	54,284, 5620	12,101, 1241
M_{SUSY}, ΔM_{SUSY}	22,331, 2229	40,968, 971.9	78,038, 3016	56,526, 5640	12,135, 1284
m_h, Δm_h	124.6, 17.0	123.5, − 2.0	**125.6**, **52.8**	**125.6**, **− 3.7**	124.1, −5.4
$\Delta a_\mu \times 10^{10}$, $\Delta(\Delta a_\mu) \times 10^{10}$	1.2, −0.1	0.2, 0.0	0.3, − 0.2	0.0, 0.0	**3.0**, **− 22.1**

5 Notes on muon anomalous magnetic moment

One of the main motivations behind this study was to analyse the NH contributions to muon $g-2$ (Δa_μ), which has been realized mostly with the enhancing effects in previous studies. Considering the previous discussions in our work; however, running the sparticles and Higgs boson to heavier masses, there was a possibility for that the NH contributions may reduce the SUSY contributions to muon $g-2$. After the recent updates on experimental [81] and theoretical [80] analyses, such a suppression might be favored. Despite the slight change from the experimental measurements, the theoretical results have provided a significant improvement by including the lattice calculations which almost remove the need for BSM contributions to muon $g-2$. The new results fit with the experimental measurements as $\Delta a_\mu \equiv \Delta a_\mu^{\text{exp}} - \Delta a_\mu^{\text{SM}} \simeq 3.8(6.6) \times 10^{-10}$, which can provide a significant negative impact in SUSY models when the smuons and Bino happen to be lighter than about 1 TeV in the spectrum.

Moreover, one of the distinctive features of the models in the GMSB-ADJ class is to accommodate large SUSY contributions to muon $g-2$ [22]. In this context, negative NH contributions to muon $g-2$ can receive special importance to fit the muon $g-2$ results with the latest measurements and SM calculations. Figure 9 displays our results for muon $g-2$ and the NH contributions to it in the $\Delta a_\mu - \Delta a_\mu^H$, $\Delta a_\mu - \tan\beta$, $\Delta(\Delta a_\mu) - A'_\mu$, and $m_{\tilde{\mu}_1} - M_{\tilde{B}}$ planes. The color coding is the same as Fig. 1. The horizontal and vertical dashed lines indicate the bound $\Delta a_\mu \leq 6.6 \times 10^{10}$ as recently reported by the White Paper (WP25) [80]. The horizontal line in the $\Delta a_\mu - \Delta a_\mu^H$ plane represents the solutions with negligible NH contributions to Δa_μ ($\Delta a_\mu = \Delta a_\mu^H$). Also, the diagonal line in the $m_{\tilde{\mu}_1} - M_{\tilde{B}}$ plane indicates the mass degeneracy between smuon and Bino ($m_{\tilde{\mu}_1} = M_{\tilde{B}}$). Note that we present the only solutions which yield physical (non-tachyonic) masses in both the NH and holomorphic cases, so the results show the NH contributions in the parameter space of the holomorphic GMSB-ADJ. As seen from the $\Delta a_\mu - \Delta a_\mu^H$ plane, one can fit the muon $g-2$ results with the NH contributions (green solutions under the horizontal dashed line), even if the holomorphic case leads to large SUSY contributions ($\Delta a_\mu^H \approx 40 \times 10^{-10}$). These results allow one to fit large $\tan\beta$ solutions as well, as shown in the $\Delta a_\mu - \tan\beta$ plane. These negative NH contributions can be investigated in terms of the NH trilinear coupling between the smuons and H_u denoted by A'_μ. The $\Delta(\Delta a_\mu) - A'_\mu$ plane shows that large A'_μ values can reduce the SUSY contributions to muon $g-2$ significantly by about 50×10^{-10}. This NH term can manage reducing the muon $g-2$ contributions by driving the smuon to heavier masses, but especially when it is negative, it also reduces the enhancement in SUSY contributions from the mixing in smuon by modifying it as $\mu \tan\beta \to (\mu + A'_\mu)\tan\beta$. With this reduction in the smuon mixing, one can still accommodate relatively light smuons and Binos in the spectrum consistently with the latest measurements and calculations of Δa_μ. The allowed mass ranges

for smuons and Binos are displayed in the $m_{\tilde{\mu}_1} - M_{\tilde{B}}$ plane of Fig. 9.

Before we conclude, we exemplify our findings with several benchmark scenarios in Table 1. All the points are selected by requiring to be consistent with the experimental constraints employed in our analyses. All the parameters, except Δa_μ, are expressed in units of GeV. Point 1 depicts a solution which involves inconsistently light staus ($\simeq$ 60 GeV) in the spectrum without the NH contributions. The NH terms are induced at the order of 10^4 GeV in such solutions, and their contributions shift the stau mass to about 6 TeV. The sbottom and stop receive about 1–2 TeV NH contributions. The SM-like Higgs boson mass is also lifted by about 17 GeV and becomes consistent with the experimental constraints. In contrast to Point1, Point 2 exemplifies the largest negative NH contributions to the stau mass which is realized in our analyses at about 275 GeV. These solutions represented by Point 2 induce the NH terms smaller by one order of magnitude in comparison with those displayed by Point 1. In addition, the $M_{\rm Mess}$ happens one order of magnitude larger. The contributions to sbottom and stop are about 20 GeV, and they are negligible compared to their masses, though the NH contributions modifies the renormalization scale ($M_{\rm SUSY}$) by about 1 TeV, which is also negligible comparing to $M_{\rm SUSY}$. The negative contributions to stau and stop in these solutions leads to about 2 GeV negative contribution in the SM-like Higgs Boson mass. Points 3 and 4 represent the SM-like Higgs boson solutions which coincide with its experimental value ($\sim$ 125.6 GeV). Point 3 display a solution in which the SM-like Higgs boson receives relatively large and positive NH contributions, and its mass is shifted from about 70 to 125.6 GeV. On the other hand, Point 4 shows negative contributions to realize 125.6 GeV Higgs boson. Such contributions are realized at about -4 GeV in our analyses. All the points except Point 4 exhibit negligible contributions to muon $g-2$ due to the heavy spectrum. Point 5, on the other hand, depicts a solution which predicts a large muon $g-2$ results in the holomorphic case, while the result fits with the current constraint on muon $g-2$ after receiving the NH contributions.

6 Conclusion

We explore the implications of the models in which the SUSY breaking is transmitted to the visible sector through the gauge interactions. In this class of models, the messenger fields reside in the adjoint representation of the MSSM gauge group, and considering the complete representation the fields do not lead to non-zero anomalies. We include the NH terms in the Lagrangian, which are induced at the third-loop level of the perturbation theory. In our case, there is no SUSY breaking singlet field, so the infinities and the hierarchy problem in the SM-like Higgs boson mass may not arise. In the framework of the GMSB-ADJ, we link such NH terms to the SUSY breaking scales, which brings a further suppression on them by $1/M_{\rm Mess}$. Despite this further suppression, we observe that such NH terms can be as large as about 200 TeV, when the SUSY breaking in the hidden sector happens at a relatively large scales, while the visible sector sees it at lower scales ($M_{\rm Mess} \lesssim 10^{11}$ GeV). Previous studies consider such terms rather in an effective approach in which they contribute to the physical observables through the mixing of the sparticles. These contributions can significantly alter the masses especially for the stau and sbottom, since they are enhanced with $\tan\beta$, while they provide minor changes in stops due to the suppression by $\tan\beta$. Besides, the Higgsino masses can be realized as $\mu + \mu'$, where μ' is induced NH Higgsino mass. Therefore, one can fit heavy Higgsino masses even in natural SUSY models. Apart from raising the masses of the sparticles and SM-like Higgs boson, they provide also significant contributions to muon $g-2$, which may receive a strong negative impact from the latest reports about its experimental measurements and theoretical calculations.

In our work, we impose the NH terms at the SUSY breaking scale in the visible sector by linking them numerically to the masses of the messengers as $A_0' \sim \Lambda_i^2/M_{\rm Mess}$, and include them in RG evolutions of the SSB parameters. The main impact, especially those from their RG contributions, is that the parameter space of the models is significantly enlarged. The small Λ_5 values mostly lead to tachyonic right-handed staus without the NH contributions, while even small NH terms can keep its mass-square positive through the RG evolutions. It allows one to explore the regions with small Λ_5. We observe that the NH contributions can differ the right-handed stau mass by about 25 TeV. This difference reduces to about 20 TeV at most when one includes their effect in stau mixing in calculating the mass eigenstates of staus. Similarly, these terms can yield heavier stop at the low scale by about 15 TeV. Such a large difference in stop masses together with staus can yield significant enhancement in the Higgs boson mass by about 80 GeV. Despite expecting large contributions for sbottoms, we realize only about 6–7 TeV difference in sbottom mass by comparing with the holomorphic case. We find that the NH contributions through the RGEs and sparticle mixing rather cancel each other. Even though we observe mostly positive contributions from the NH terms, in a small region these contributions can slightly lower the mass spectrum by about 1 TeV. In these regions, also the SM-like Higgs mass decreases by about 20 GeV.

An interesting effect from the NH contributions can be seen in the SUSY contributions to muon $g-2$. The latest measurements strengthen the consensus that the SM may not need BSM contributions to fit its predictions on muon $g-2$ with the experimental measurements. A negative impact from the latest status of muon $g-2$ may exclude the light slepton

and gaugino solutions. One can expect that the NH contributions suppress the SUSY contributions to muon $g-2$, since they drive the SUSY particles heavier masses in most of the parameter space. However, this observation still excludes the light sparticles. On the other hand, the NH terms do not only alter the muon $g-2$ results by raising the sparticle masses. They directly contribute to the muon $g-2$ through smuon mixing, and these contributions are enhanced by $\tan\beta$. In our analyses, we realize mostly negative contributions to muon $g-2$ in the experimentally consistent regions (green in the plots), and they can even change the muon $g-2$ results by about -50×10^{-10}. In this context, the large muon $g-2$ solutions in the holomorphic case can be fit with the current measurements and calculations after including the NH contributions. Consequently, the light sparticle and gaugino solutions can still survive.

Acknowledgements The work represented in this study is supported by the Scientific and Technological Research Council of Turkey (TUBITAK) Grant No. MFAG-124F280. The numerical calculations reported in this paper were partially performed at TUBITAK ULAKBIM, High Performance and Grid Computing Center (TRUBA resources).

Data Availability Statement This manuscript has no associated data. [Authors' comment: The data that support the findings of this article are not publicly available. The data are available from the authors upon reasonable request.]

Code Availability Statement Code/software will be made available on reasonable request. [Authors' comment: The numerical packages used in the analyses of this article are publicly available and addressed properly. The auxiliary codes are also provided as the supplementary files.]

Open Access This article is licensed under a Creative Commons Attribution 4.0 International License, which permits use, sharing, adaptation, distribution and reproduction in any medium or format, as long as you give appropriate credit to the original author(s) and the source, provide a link to the Creative Commons licence, and indicate if changes were made. The images or other third party material in this article are included in the article's Creative Commons licence, unless indicated otherwise in a credit line to the material. If material is not included in the article's Creative Commons licence and your intended use is not permitted by statutory regulation or exceeds the permitted use, you will need to obtain permission directly from the copyright holder. To view a copy of this licence, visit http://creativecommons.org/licenses/by/4.0/.
Funded by SCOAP[3].

References

1. ATLAS collaboration, Observation of a new particle in the search for the standard model Higgs boson with the ATLAS detector at the LHC. Phys. Lett. B **716**, 1 (2012). https://doi.org/10.1016/j.physletb.2012.08.020. arXiv:1207.7214
2. CMS collaboration, Observation of a new boson at a mass of 125 GeV with the CMS experiment at the LHC. Phys. Lett. B **716**, 30 (2012). https://doi.org/10.1016/j.physletb.2012.08.021. arXiv:1207.7235
3. CMS collaboration, Observation of a new boson with mass near 125 GeV in pp collisions at $\sqrt{s}=7$ and 8 TeV. JHEP **06**, 081 (2013). https://doi.org/10.1007/JHEP06(2013)081. arXiv:1303.4571
4. G. Degrassi, S. Di Vita, J. Elias-Miro, J.R. Espinosa, G.F. Giudice, G. Isidori et al., Higgs mass and vacuum stability in the standard model at NNLO. JHEP **08**, 098 (2012). https://doi.org/10.1007/JHEP08(2012)098. arXiv:1205.6497
5. F. Bezrukov, M.Y. Kalmykov, B.A. Kniehl, M. Shaposhnikov, Higgs boson mass and new physics. JHEP **10**, 140 (2012). https://doi.org/10.1007/JHEP10(2012)140. arXiv:1205.2893
6. D. Buttazzo, G. Degrassi, P.P. Giardino, G.F. Giudice, F. Sala, A. Salvio et al., Investigating the near-criticality of the Higgs boson. JHEP **12**, 089 (2013). https://doi.org/10.1007/JHEP12(2013)089. arXiv:1307.3536
7. M. Carena, S. Gori, I. Low, N.R. Shah, C.E.M. Wagner, Vacuum stability and Higgs diphoton decays in the MSSM. JHEP **02**, 114 (2013). https://doi.org/10.1007/JHEP02(2013)114. arXiv:1211.6136
8. M. Carena, S. Gori, N.R. Shah, C.E.M. Wagner, A 125 GeV SM-like Higgs in the MSSM and the $\gamma\gamma$ rate. JHEP **03**, 014 (2012). https://doi.org/10.1007/JHEP03(2012)014. arXiv:1112.3336
9. M.A. Ajaib, I. Gogoladze, F. Nasir, Q. Shafi, Revisiting mGMSB in light of a 125 GeV Higgs. Phys. Lett. B **713**, 462 (2012). https://doi.org/10.1016/j.physletb.2012.06.036. arXiv:1204.2856
10. I. Gogoladze, A. Mustafayev, Q. Shafi, C.S. Un, Yukawa unification and sparticle spectroscopy in gauge mediation models. Phys. Rev. D **91**, 096005 (2015). https://doi.org/10.1103/PhysRevD.91.096005. arXiv:1501.07290
11. Particle Data Group collaboration, Review of particle physics. Phys. Rev. D **110**, 030001 (2024). https://doi.org/10.1103/PhysRevD.110.030001
12. M.D. Goodsell, K. Nickel, F. Staub, Two-Loop Higgs mass calculations in supersymmetric models beyond the MSSM with SARAH and SPheno. Eur. Phys. J. C **75**, 32 (2015). https://doi.org/10.1140/epjc/s10052-014-3247-y. arXiv:1411.0675
13. B.C. Allanach, SOFTSUSY: a program for calculating supersymmetric spectra. Comput. Phys. Commun. **143**, 305 (2002). https://doi.org/10.1016/S0010-4655(01)00460-X. arXiv:hep-ph/0104145
14. B.C. Allanach, A. Bednyakov, R. Ruiz de Austri, Higher order corrections and unification in the minimal supersymmetric standard model: SOFTSUSY3.5. Comput. Phys. Commun. **189**, 192 (2015). https://doi.org/10.1016/j.cpc.2014.12.006. arXiv:1407.6130
15. H. Baer, V. Barger, D. Martinez, Comparison of SUSY spectra generators for natural SUSY and string landscape predictions. Eur. Phys. J. C **82**, 172 (2022). https://doi.org/10.1140/epjc/s10052-022-10141-2. arXiv:2111.03096
16. M.E. Gomez, Q. Shafi, A. Tiwari, C.S. Un, Muon $\mathbf{g-2}$, neutralino dark matter and stau NLSP. Eur. Phys. J. C **82**, 561 (2022). https://doi.org/10.1140/epjc/s10052-022-10507-6. arXiv:2202.06419
17. I. Gogoladze, Q. Shafi, C.S. Ün, Reconciling the muon g−2, a 125 GeV Higgs boson, and dark matter in gauge mediation models. Phys. Rev. D **92**, 115014 (2015). https://doi.org/10.1103/PhysRevD.92.115014. arXiv:1509.07906
18. T. Han, T. Yanagida, R.-J. Zhang, Adjoint messengers and perturbative unification at the string scale. Phys. Rev. D **58**, 095011 (1998). https://doi.org/10.1103/PhysRevD.58.095011. arXiv:hep-ph/9804228
19. G. Bhattacharyya, B. Bhattacherjee, T.T. Yanagida, N. Yokozaki, A practical GMSB model for explaining the muon (g-2) with gauge coupling unification. Phys. Lett. B **730**, 231 (2014). https://doi.org/10.1016/j.physletb.2013.12.064. arXiv:1311.1906
20. G. Bhattacharyya, T.T. Yanagida, N. Yokozaki, Focus point gauge mediation with incomplete adjoint messengers and gauge coupling unification. Phys. Lett. B **749**, 82 (2015). https://doi.org/10.1016/j.physletb.2015.07.052. arXiv:1506.05962

21. I. Gogoladze, A. Mustafayev, Q. Shafi, C.S. Un, Gauge mediation models with adjoint messengers. Phys. Rev. D **94**, 075012 (2016). https://doi.org/10.1103/PhysRevD.94.075012. arXiv:1609.02124
22. I. Gogoladze, C.S. Un, Muon g - 2 in gauge mediated supersymmetry breaking models with adjoint messengers. Phys. Rev. D **95**, 035028 (2017). https://doi.org/10.1103/PhysRevD.95.035028. arXiv:1612.02376
23. K. Inoue, A. Kakuto, H. Komatsu, S. Takeshita, Aspects of grand unified models with softly broken supersymmetry. Prog. Theor. Phys. **68**, 927 (1982). https://doi.org/10.1143/PTP.68.927
24. L.J. Hall, L. Randall, Weak scale effective supersymmetry. Phys. Rev. Lett. **65**, 2939 (1990). https://doi.org/10.1103/PhysRevLett.65.2939
25. J. Bagger, E. Poppitz, Destabilizing divergences in supergravity coupled supersymmetric theories. Phys. Rev. Lett. **71**, 2380 (1993). https://doi.org/10.1103/PhysRevLett.71.2380. arXiv:hep-ph/9307317
26. J. Bagger, E. Poppitz, L. Randall, Destabilizing divergences in supergravity theories at two loops. Nucl. Phys. B **455**, 59 (1995). https://doi.org/10.1016/0550-3213(95)00463-3. arXiv:hep-ph/9505244
27. S.P. Martin, Dimensionless supersymmetry breaking couplings, flat directions, and the origin of intermediate mass scales. Phys. Rev. D **61**, 035004 (2000). https://doi.org/10.1103/PhysRevD.61.035004. arXiv:hep-ph/9907550
28. I. Jack, D.R.T. Jones, Nonstandard soft supersymmetry breaking. Phys. Lett. B **457**, 101 (1999). https://doi.org/10.1016/S0370-2693(99)00530-4. arXiv:hep-ph/9903365
29. I. Jack, D.R.T. Jones, Quasiinfrared fixed points and renormalization group invariant trajectories for nonholomorphic soft supersymmetry breaking. Phys. Rev. D **61**, 095002 (2000). https://doi.org/10.1103/PhysRevD.61.095002. arXiv:hep-ph/9909570
30. H.E. Haber, J.D. Mason, Hard supersymmetry-breaking 'wrong-Higgs' couplings of the MSSM. Phys. Rev. D **77**, 115011 (2008). https://doi.org/10.1103/PhysRevD.77.115011. arXiv:0711.2890
31. U. Chattopadhyay, D. Das, S. Mukherjee, Exploring non-holomorphic soft terms in the framework of gauge mediated supersymmetry breaking. JHEP **01**, 158 (2018). https://doi.org/10.1007/JHEP01(2018)158. arXiv:1710.10120
32. M.I. Ali, M. Chakraborti, U. Chattopadhyay, S. Mukherjee, Muon and electron $(g-2)$ anomalies with non-holomorphic interactions in MSSM. Eur. Phys. J. C **83**, 60 (2023). https://doi.org/10.1140/epjc/s10052-023-11216-4. arXiv:2112.09867
33. S. Chakraborty, T.S. Roy, Radiatively generated source of flavor universal scalar soft masses. Phys. Rev. D **100**, 035020 (2019). https://doi.org/10.1103/PhysRevD.100.035020. arXiv:1904.10144
34. C.S. Ün, c.H. Tanyıldızı, S. Kerman, L. Solmaz, Generalized soft breaking leverage for the MSSM. Phys. Rev. D **91**, 105033 (2015). https://doi.org/10.1103/PhysRevD.91.105033. arXiv:1412.1440
35. M. Rehman, S. Heinemeyer, Nonholomorphic soft-term contributions to the Higgs-boson masses in the Feynman diagrammatic approach. Phys. Rev. D **107**, 095033 (2023). https://doi.org/10.1103/PhysRevD.107.095033. arXiv:2212.13757
36. C.S. Un, Low fine-tuning with heavy higgsinos in Yukawa unified SUSY GUTs. Turk. J. Phys. **48**, 1 (2024). https://doi.org/10.55730/1300-0101.2753. arXiv:2308.12862
37. S. Israr, M.E. Gómez, M. Rehman, Nonholomorphic higgsino mass term effects on muon g − 2 and dark matter relic density in flavor symmetry-based minimal supersymmetric standard model. Particles **8**, 30 (2025). https://doi.org/10.3390/particles8010030
38. S. Israr, M. Rehman, Higgs decay to $Z\gamma$ in the minimal supersymmetric standard model and its nonholomorphic extension. Eur. Phys. J. Plus **140**, 397 (2025). https://doi.org/10.1140/epjp/s13360-025-06401-1. arXiv:2407.01210
39. M. Rehman, S. Heinemeyer, Lepton flavor violation in nonholomorphic soft SUSY-breaking scenarios: experimental limits and excesses. Eur. Phys. J. C **85**, 638 (2025). https://doi.org/10.1140/epjc/s10052-025-14371-y. arXiv:2411.00479
40. M. Rehman, S. Heinemeyer, Toward a refined understanding of nonholomorphic soft SUSY-breaking effects on the Higgs boson mass spectra. Phys. Rev. D **111**, 115027 (2025). https://doi.org/10.1103/n5tq-1h1y. arXiv:2504.11891
41. K. Hamaguchi, M. Ibe, T.T. Yanagida, N. Yokozaki, Testing the minimal direct gauge mediation at the LHC. Phys. Rev. D **90**, 015027 (2014). https://doi.org/10.1103/PhysRevD.90.015027. arXiv:1403.1398
42. A. Delgado, M. Garcia, M. Quiros, Electroweak and supersymmetry breaking from the Higgs boson discovery. Phys. Rev. D **90**, 015016 (2014). https://doi.org/10.1103/PhysRevD.90.015016. arXiv:1312.3235
43. P. Draper, P. Meade, M. Reece, D. Shih, Implications of a 125 GeV Higgs for the MSSM and low-scale SUSY breaking. Phys. Rev. D **85**, 095007 (2012). https://doi.org/10.1103/PhysRevD.85.095007. arXiv:1112.3068
44. P. Draper, G. Lee, C.E.M. Wagner, Precise estimates of the Higgs mass in heavy supersymmetry. Phys. Rev. D **89**, 055023 (2014). https://doi.org/10.1103/PhysRevD.89.055023. arXiv:1312.5743
45. G.F. Giudice, R. Rattazzi, Theories with gauge mediated supersymmetry breaking. Phys. Rep. **322**, 419 (1999). https://doi.org/10.1016/S0370-1573(99)00042-3. arXiv:hep-ph/9801271
46. P. McGuirk, G. Shiu, F. Ye, Soft branes in supersymmetry-breaking backgrounds. JHEP **07**, 188 (2012). https://doi.org/10.1007/JHEP07(2012)188. arXiv:1206.0754
47. S.P. Martin, A supersymmetry primer. Adv. Ser. Direct. High Energy Phys. **18**, 1 (1998). https://doi.org/10.1142/9789812839657_0001. arXiv:hep-ph/9709356
48. T. Kitahara, T. Yoshinaga, Stau with large mass difference and enhancement of the Higgs to diphoton decay rate in the MSSM. JHEP **05**, 035 (2013). https://doi.org/10.1007/JHEP05(2013)035. arXiv:1303.0461
49. D. Bellisai, F. Fucito, M. Matone, G. Travaglini, Nonholomorphic terms in N=2 SUSY Wilsonian actions and the renormalization group equation. Phys. Rev. D **56**, 5218 (1997). https://doi.org/10.1103/PhysRevD.56.5218. arXiv:hep-th/9706099
50. L. Bergamin, P. Minkowski, SUSY glue balls, dynamical symmetry breaking and nonholomorphic potentials. arXiv:hep-th/0301155
51. W. Porod, SPheno, a program for calculating supersymmetric spectra, SUSY particle decays and SUSY particle production at e+ e- colliders. Comput. Phys. Commun. **153**, 275 (2003). https://doi.org/10.1016/S0010-4655(03)00222-4. arXiv:hep-ph/0301101
52. F. Staub, SARAH (2008). arXiv:0806.0538
53. H. Baer, S. Kraml, H. Summy, Dark matter allowed scenarios for Yukawa-unified SO(10) SUSY GUTs. JHEP **03**, 056 (2008). https://doi.org/10.1088/1126-6708/2008/03/056. arXiv:0801.1831
54. H. Baer, S. Kraml, S. Sekmen, H. Summy, Dark matter allowed scenarios for Yukawa-unified SO(10) SUSY GUTs. JHEP **03**, 056 (2008). https://doi.org/10.1088/1126-6708/2008/03/056. arXiv:0801.1831
55. G. Belanger, F. Boudjema, A. Pukhov, R.K. Singh, Constraining the MSSM with universal gaugino masses and implication for searches at the LHC. JHEP **11**, 026 (2009). https://doi.org/10.1088/1126-6708/2009/11/026. arXiv:0906.5048
56. Particle Data Group collaboration, Review of particle physics. Chin. Phys. C **38**, 090001 (2014). https://doi.org/10.1088/1674-1137/38/9/090001
57. ATLAS collaboration, Search for squarks and gluinos in final states with one isolated lepton, jets, and missing transverse momentum at $\sqrt{s} = 13$ with the ATLAS detector. Eur. Phys. J. C **81**,

600 (2021). https://doi.org/10.1140/epjc/s10052-021-09748-8. arXiv:2101.01629
58. ATLAS collaboration, Search for squarks and gluinos in final states with jets and missing transverse momentum using 139 fb^{-1} of $\sqrt{s}$ =13 TeV pp collision data with the ATLAS detector. JHEP **02**, 143 (2021). https://doi.org/10.1007/JHEP02(2021)143. arXiv:2010.14293
59. ATLAS collaboration, SUSY Summary Plots March, ATL-PHYS-PUB-2022-013 (2022)
60. Belle-II collaboration, Measurement of the photon-energy spectrum in inclusive $B \to X_s\gamma$ decays identified using hadronic decays of the recoil B meson in 2019–2021 Belle II data, BELLE2-CONF-PH-2022-018 (2022). arXiv:2210.10220
61. CMS Collaboration, Combination of the ATLAS, CMS and LHCb results on the $B^0_{(s)} \to \mu^+\mu^-$ decays, CMS-PAS-BPH-20-003 (2020)
62. B.C. Allanach, A. Djouadi, J.L. Kneur, W. Porod, P. Slavich, Precise determination of the neutral Higgs boson masses in the MSSM. JHEP **09**, 044 (2004). https://doi.org/10.1088/1126-6708/2004/09/044. arXiv:hep-ph/0406166
63. H. Bahl, S. Heinemeyer, W. Hollik, G. Weiglein, Theoretical uncertainties in the MSSM Higgs boson mass calculation. Eur. Phys. J. C **80**, 497 (2020). https://doi.org/10.1140/epjc/s10052-020-8079-3. arXiv:1912.04199
64. E. Bagnaschi, J. Pardo Vega, P. Slavich, Improved determination of the Higgs mass in the MSSM with heavy superpartners. Eur. Phys. J. C **77**, 334 (2017). https://doi.org/10.1140/epjc/s10052-017-4885-7. arXiv:1703.08166
65. P. Athron, J.-H. Park, T. Steudtner, D. Stöckinger, A. Voigt, Precise Higgs mass calculations in (non-)minimal supersymmetry at both high and low scales. JHEP **01**, 079 (2017). https://doi.org/10.1007/JHEP01(2017)079. arXiv:1609.00371
66. P. Drechsel, R. Gröber, S. Heinemeyer, M.M. Muhlleitner, H. Rzehak, G. Weiglein, Higgs-Boson masses and mixing matrices in the NMSSM: analysis of on-shell calculations. Eur. Phys. J. C **77**, 366 (2017). https://doi.org/10.1140/epjc/s10052-017-4932-4. arXiv:1612.07681
67. Slavich, P., Heinemeyer, S., Bagnaschi, E. et al.: Higgs-mass predictions in the MSSM and beyond. Eur. Phys. J. C 81, 450 (2021). https://doi.org/10.1140/epjc/s10052-021-09198-2
68. H. Bahl, I. Sobolev, G. Weiglein, The light MSSM Higgs boson mass for large $\tan\beta$ and complex input parameters. Eur. Phys. J. C **80**, 1063 (2020). https://doi.org/10.1140/epjc/s10052-020-08637-w. arXiv:2009.07572
69. R.V. Harlander, J. Klappert, A. Voigt, Higgs mass prediction in the MSSM at three-loop level in a pure $\overline{\text{DR}}$ context. Eur. Phys. J. C **77**, 814 (2017). https://doi.org/10.1140/epjc/s10052-017-5368-6. arXiv:1708.05720
70. R.V. Harlander, J. Klappert, A.D. Ochoa Franco, A. Voigt, The light CP-even MSSM Higgs mass resummed to fourth logarithmic order. Eur. Phys. J. C **78**, 874 (2018). https://doi.org/10.1140/epjc/s10052-018-6351-6. arXiv:1807.03509
71. F. Staub, W. Porod, Improved predictions for intermediate and heavy supersymmetry in the MSSM and beyond. Eur. Phys. J. C **77**, 338 (2017). https://doi.org/10.1140/epjc/s10052-017-4893-7. arXiv:1703.03267
72. H. Bahl, T. Hahn, S. Heinemeyer, W. Hollik, S. Paßehr, H. Rzehak et al., Precision calculations in the MSSM Higgs-boson sector with FeynHiggs 2.14. Comput. Phys. Commun. **249**, 107099 (2020). https://doi.org/10.1016/j.cpc.2019.107099. arXiv:1811.09073
73. S.R. Choudhury, N. Gaur, Dileptonic decay of B(s) meson in SUSY models with large tan Beta. Phys. Lett. B **451**, 86 (1999). https://doi.org/10.1016/S0370-2693(99)00203-8. arXiv:hep-ph/9810307
74. K.S. Babu, C.F. Kolda, Higgs mediated $B^0 \to \mu^+\mu^-$ in minimal supersymmetry. Phys. Rev. Lett. **84**, 228 (2000). https://doi.org/10.1103/PhysRevLett.84.228. arXiv:hep-ph/9909476
75. H. Bahl, T. Biekötter, S. Heinemeyer, C. Li, S. Paasch, G. Weiglein et al., HiggsTools: BSM scalar phenomenology with new versions of HiggsBounds and HiggsSignals. Comput. Phys. Commun. **291**, 108803 (2023). https://doi.org/10.1016/j.cpc.2023.108803. arXiv:2210.09332
76. H.E. Haber, D. O'Neil, Basis-independent methods for the two-Higgs-doublet model III: the CP-conserving limit, custodial symmetry, and the oblique parameters S, T, U. Phys. Rev. D **83**, 055017 (2011). https://doi.org/10.1103/PhysRevD.83.055017. arXiv:1011.6188
77. W. Grimus, L. Lavoura, O.M. Ogreid, P. Osland, The oblique parameters in multi-Higgs-doublet models. Nucl. Phys. B **801**, 81 (2008). https://doi.org/10.1016/j.nuclphysb.2008.04.019. arXiv:0802.4353
78. CDF collaboration, High-precision measurement of the W boson mass with the CDF II detector. Science **376**, 170 (2022). https://doi.org/10.1126/science.abk1781
79. CMS collaboration, High-precision measurement of the W boson mass with the CMS experiment at the LHC. arXiv:2412.13872
80. R. Aliberti et al., The anomalous magnetic moment of the muon in the Standard Model: an update. arXiv:2505.21476
81. Muon g-2 collaboration, Measurement of the Positive Muon Anomalous Magnetic Moment to 127 ppb. arXiv:2506.03069
82. CMS collaboration, Searches for additional Higgs bosons and for vector leptoquarks in $\tau\tau$ final states in proton-proton collisions at $\sqrt{s}$ = 13 TeV. JHEP **07**, 073 (2023). https://doi.org/10.1007/JHEP07(2023)073. arXiv:2208.02717
83. ATLAS collaboration, Search for heavy Higgs bosons decaying into two tau leptons with the ATLAS detector using pp collisions at $\sqrt{s} = 13$ TeV. Phys. Rev. Lett. **125**, 051801 (2020). https://doi.org/10.1103/PhysRevLett.125.051801. arXiv:2002.12223